2',7'-dichlorofluorescin-based analysis of Fenton chemistry reveals auto-amplification of probe fluorescence and albumin as catalyst for the detection of hydrogen peroxide

Teresa Gonzalez, Franck Peiretti, Catherine Defoort, Patrick Borel, Roland Govers

Analysis of the Fenton reaction by 2',7'-dichlorofluorescin reveals hydroxyl radical-induced auto-amplification of probe fluorescence and albumin as a catalyst for the detection of hydrogen peroxide

Teresa Gonzalez, Franck Peiretti, Catherine Defoort, Patrick Borel, and Roland Govers *

Aix Marseille University, INSERM, INRAE, C2VN, 13385 Marseille, France

Teresa.Gonzalez@univ-amu.fr
Franck.Peiretti@univ-amu.fr
Catherine.Defoort@univ-amu.fr
Patrick.Borel@univ-amu.fr

* Corresponding author; Roland.Govers@univ-amu.fr

ABSTRACT

Fluorophore 2',7'-dichlorofluorescin (DCF) is the most frequently used probe for measuring oxidative stress in cells, but many aspects of DCF remain to be revealed. Here, DCF was used to study the Fenton reaction in detail, which confirmed that in a cell-free system, the hydroxyl radical was easily measured by DCF, accompanied by the consumption of H_2O_2 and the conversion of ferrous iron into ferric iron. DCF fluorescence was more specific for hydroxyl radicals than the measurement of thiobarbituric acid (TBA)-reactive 2-deoxy-D-ribose degradation products, which also detected H_2O_2. As expected, hydroxyl radical-induced DCF fluorescence was inhibited by iron chelation, anti-oxidants, and hydroxyl radical scavengers and enhanced by low concentrations of ascorbate. Remarkably, due to DCF fluorescence auto-amplification, Fenton reaction-induced DCF fluorescence steadily increased in time even when all ferrous iron was oxidized. Surprisingly, the addition of bovine serum albumin rendered DCF sensitive to H_2O_2 as well. Within cells, DCF appeared not to react directly with H_2O_2 but indirect via the formation of hydroxyl radicals, since H_2O_2-induced cellular DCF fluorescence was fully abolished by iron chelation and hydroxyl radical scavenging. Iron chelation in H_2O_2-stimulated cells in which DCF fluorescence was already increasing did not abrogate further increases in fluorescence, suggesting DCF fluorescence auto-amplification in cells. Collectively, these data demonstrate that DCF is a very useful probe to detect hydroxyl radicals and hydrogen peroxide and to study Fenton chemistry, both in test tubes as well as in intact cells, and that fluorescence auto-amplification is an intrinsic property of DCF.

Introduction

Reactive oxygen species (ROS) are essential for every living organism. At physiological concentrations, they have unique beneficial functions and are part of host defense mechanisms, act as second messengers, and play a role in day-to-day chemical reactions. A highly coordinated equilibrium exists between the generation of ROS and antioxidant systems. Antioxidants and enzymes that display antioxidant activity serve to keep down the levels of free radicals, permitting them to perform essential biological functions without too much damage. However, under certain pathophysiological conditions, these systems may be in disequilibrium, leading to a significant increase in ROS levels and a situation of oxidative stress. This is accompanied by oxidation of proteins, lipids and DNA, and hence, in a change in their physiological roles. Substantial increases in ROS and oxidative damage have been demonstrated to play important roles in the development of several pathologies, including diabetes, cancer, and cardiovascular and neurodegenerative diseases and in aging [1].

One of the chemical reactions that can play a role in the generation of oxidative stress is the Fenton reaction [1]. Bivalent (ferrous) iron and hydrogen peroxide participate in this reaction, leading to the production of the hydroxyl radical ($^{\bullet}OH$), according to the following reaction:

$$Fe^{2+} + H_2O_2 \rightarrow Fe^{3+} + {}^{\bullet}OH + OH^{-}$$

The highly toxic hydroxyl radical is considered to play major roles in a variety of diseases and in the aging process and to be the most reactive of all ROS. Hence, it quickly reacts with proteins, lipids, DNA and other molecules that are in close proximity of the place where the radical is generated. In addition to its native role in biological systems, the Fenton reaction has also been applied as an oxidizing process for destroying hazardous organics, amongst others for wastewater treatment and remediation of groundwater (e.g. pesticides, aromatic amines, surfactants), because of the extreme reactivity of the hydroxyl radical [2,3]. This reactivity renders its half-life extremely short and its diffusion distance very limited. For this reason, measuring hydroxyl radical levels is challenging. Relative levels of hydroxyl radicals, generated through Fenton chemistry, have been estimated *in vitro* by various methodologies: (i) Electron Spin Resonance (ESR) using spin traps DMPO [4-6] and PBN [7,8]; (ii) by measuring thiobarbituric acid-reactive signal (TBARS) using micelles [9], liposomes [10,11], or 2-deoxy-D-ribose [12-14]; (iii) DNA nicking (single strand breaks in double strand DNA), requiring agarose gel electrophoresis to display differential migration patterns [8,13,15]; (iv) the reaction of hydroxyl radicals with salicylate, forming 2,3-dihydroxy-benzoic acid (DHBA), requiring HPLC analysis [15-17]; (v) hydroxyl radical-mediated oxidation of 2',7'-dichlorodihydrofluorescein, resulting in the formation of the highly fluorescent 2',7'-dichlorofluorescein [6,18-20].

The molecule 2',7'-dichlorodihydrofluorescein (also known as 2',7'-dichlorofluorescin, and abbreviated as DCFH and $DCFH_2$) is by far the most frequently used probe for measuring ROS. In the presence of ROS, it is oxidized into fluorescent 2',7'-dichlorofluorescein (DCF). In cell cultures, 2',7'-dichlorodihydrofluorescein is used as 2',7'-dichlorodihydrofluorescein diacetate or DCF-DA, also known as DCFH-DA and

$DCFH_2$-DA (throughout the current study abbreviated as DCF for the sake of simplicity). $DCFH_2$-DA enters the cells and accumulates mostly in the cytosol, where it is deacetylated by esterases into $DCFH_2$ which has been suggested to somewhat limit the diffusion of the molecule out of the cell (Suppl. Fig. S1). Subsequently, it may be oxidized by ROS. Its reactivity towards various ROS has been a debate for decades. Paradoxically, while initially developed to detect hydrogen peroxide (H_2O_2) [21], it is now generally accepted that DCF is unlikely to react significantly with H_2O_2 [18,19,22,23]. DCF has been demonstrated to be oxidized by peroxyl radicals ($RO_2^{\bullet}$), alkoxyl radicals ($RO^{\bullet}$), nitrogen dioxide radicals ($NO_2^{\bullet}$), carbonate radicals ($CO_3^{\bullet-}$), peroxynitrite ($ONOO^-$), hypochlorous acid (HOCl), and hydroxyl radicals ($^{\bullet}OH$) [1,18,20,22,24]. The non-discriminatory nature of DCF concerning its sensitivity to various oxidizing molecules may somewhat limit its use, but at the same time it turns DCF into a highly valuable probe for studying general cellular oxidative stress and redox-sensitive toxicological phenomena. While the Fenton reaction-generated hydroxyl radical is known to oxidize DCF [6,18-20], there are only a few detailed studies on the use of DCF for the analysis of the Fenton reaction in cell-free systems, in particular in combination with measurements of H_2O_2 and iron concentrations. Also for intact cells, only little information is available on the analysis of Fenton chemistry, H_2O_2, and hydroxyl radicals by DCF, even though this probe has been extensively used in many cell systems. Hence, many aspects of the DCF-mediated analysis of Fenton chemistry remain to be revealed.

In the present investigation, we have studied DCF for the analysis of Fenton chemistry and the detection of hydroxyl radicals. We demonstrate that, dependent on reaction conditions, DCF can be used as a detector for hydroxyl radicals (in the absence or presence of H_2O_2), for H_2O_2 (in the absence of hydroxyl radicals), and for oxidative stress induced by the combination of hydroxyl radicals and H_2O_2. Under certain conditions, DCF auto-amplifies its own fluorescence, while BSA acts as a catalyst, enabling the oxidation of DCF by H_2O_2. Within cells, DCF also auto-amplifies its fluorescence but does not react with H_2O_2.

Materials and Methods

Reagents

Mannitol, dimethylthiourea, and HRP were from Santa Cruz (Heidelberg, Germany). Rotenone, ferrozine, Iron(II) sulphate heptahydrate ($FeSO_4 \bullet 7H_2O$), Iron(III) chloride hexahydrate ($FeCl_3 \bullet 6H_2O$), BHA, ascorbic acid, bovine and rabbit IgG, alcohol dehydrogenase, lysozyme, RNase A, trolox, DTPA, EDTA, PNT, harman, 2-deoxy-D-ribose, thiobarbituric acid, neocuproine, catalase and H_2O_2 were from Sigma-Aldrich (Saint-Quentin Fallavier, France). OPD and $DCFH_2$-DA were from Euromedex (Souffelweyersheim, France). 3T3-L1 preadipocytes were obtained from the American Type Culture Collection ATCC/LGC Standards (Molsheim, France). Fetal bovine serum (South American origin) was from D. Dutscher (Brumath, France). Culture media were from Invitrogen (Cergy Pontoise, France). BSA batches were obtained from Euromedex (batch I) or Sigma (batches II-V). Batch I (#04100811C) was prepared by heat shock, purity ≥98%. Batch II (#A7906) was prepared by heat shock, purity ≥98%. Batch III (#A7030) was prepared by heat shock, essentially FFA- and globulin-free, protease-free, purity ≥98%. Batch IV (#A6003) was prepared using cold ethanol, essentially FFA-free, purity ≥96%. Batch V (#A7511) was prepared using cold ethanol, essentially FFA-free, purity ≥97%. Unless stated otherwise, BSA batch I was used for experiments.

Cell-free DCF assay

DCF experiments were performed using black 96 well plates and Ringer-based assay buffer, containing 150 mM NaCl, 5 mM KCl, 1 mM $CaCl_2$, 1 mM $MgCl_2$, 1.25 mM $MgSO_4$, 25 mM glucose, 50 mM HEPES pH 7.4, supplemented with 5 µM $DCFH_2$-DA (Suppl. Fig. S1). When indicated, 0.2% w/v BSA was added. Generally, one solution was deposited in the wells and an equal volume of a second solution was added to start the reaction. Hydrogen peroxide was always present in the second solution. DMSO concentrations were always equal between all wells (at a maximum concentration of 1% v/v). Kinetics of fluorescence intensities were analyzed at 37°C using a fluorescence microtitre plate reader (Fluostar Optima, BMG Labtechnologies, Offenburg, Germany) and excitation /emission filters 485 nm/520 nm. The increase in DCF fluorescence from 0 to 30 min was used as estimate for ROS levels, unless stated otherwise. In case the experiments involved ascorbate, ROS intensity from Fenton chemistry was estimated from the first 7.5 min window, to avoid interference from the reaction of ascorbate with H_2O_2. Of note, concentrations of ascorbate up to 1 mM did not change the pH of the Ringer buffer.

Hydrogen peroxide assay

H_2O_2 assays were performed in transparent 96 well plates. Samples and standards were in Ringer-based assay buffer (see above) and contained up to 100 µM H_2O_2. To 120 µl of sample or standard, 5 µl of 37.5 mM EDTA was added to stop the Fenton reaction and 31 µl of a 5x concentrated H_2O_2 assay reagent, containing 0.5 mg/ml HRP substrate OPD and 5 µg/ml HRP in 250 mM tris pH 8.8. Absorbance at 450 nm was immediately measured using microtitre plate reader BMG Fluostar Optima (BMG Labtechnologies, Offenburg, Germany).

Iron (Fe^{2+}/Fe^{3+}) assay

Iron concentrations were determined in transparent 96 well plates using ferrozine [25]. For samples and standards, various concentrations of Fe^{2+}/Fe^{3+} were prepared in 20 mM HCl. Subsequently, these iron stocks were diluted 20 times in Ringer-based assay buffer (see above), resulting in a final HCl concentration of 1 mM in samples and standards. Samples were subjected to various incubations as required. Subsequently, to 90 µl of samples and standards, 30 µl of 500 mM KAc pH 5.5/2.5 mM neocuproine was added and 30 µl of 6 mM ferrozine. Absorbance at 560 nm was measured immediately using microtitre plate reader BMG Fluostar Optima (BMG Labtechnologies, Offenburg, Germany). Subsequently, 30 µl of 600 mM ascorbate was added and absorbance was measured immediately and also after 60 min at 37°C. The first measurement was used to determine Fe^{2+} levels and the difference in absorbance between the second and third measurement was used to calculate Fe^{3+} concentrations.

TBARS assay for the detection of hydroxyl radicals

The TBARS assay was applied essentially as described elsewhere [11,13]. Samples were prepared using Ringer-based assay buffer (see above) and contained 10 mM 2-deoxy-D-ribose, H_2O_2, and Fe^{2+}/Fe^{3+}. Samples were incubated for 30 or 120 min at 37°C. To 200 µl of assay samples, 200 µl of 1% thiobarbituric acid (TBA) in 50 mM NaOH was added, immediately followed by the addition of 200 µl of 2.8% trichloroacetic acid (TCA). After incubating for 15 min at 100°C, samples were cooled down for 10 min on ice and centrifuged for 10 min at 21,500 g. Absorbance at 544 nm was analyzed for 200 µl of the supernatants using a BMG Fluostar Optima microtitre plate reader (BMG Labtechnologies, Offenburg, Germany).

DTNB assay for the determination of free thiol groups in albumin

Albumin contains a single free thiol group at Cys34 (all other Cys residues form intramolecular disulfide bonds) [26]. An oxidative environment results in oxidation of albumin Cys-34 and thus in a reduction in the number of free thiol groups [27]. DTNB (5,5'-dithiobis-(2-nitrobenzoic acid, also known as Ellman's reagent) was used to measure relative amounts of free thiol groups in BSA solutions [28,29]. BSA batch III was used for thiol measurements since this BSA did not contain free fatty acids (FFAs) that might interfere with the assay. To samples containing up to 1% (w/v) BSA (corresponding to 150 µM), DTNB was added at a concentration of 1 mM. Absorbance at 405 nm was measured using a BMG Fluostar Optima microtitre plate reader (BMG Labtechnologies, Offenburg, Germany) and background absorbance was subtracted. DTNB absorbance of non-oxidized BSA was linear up to 1% BSA (not shown).

Cell culture and cellular DCF assay

Adipocytes were used as cell model, since these cells are known to respond to hydrogen peroxide [30,31]. 3T3-L1 preadipocytes were cultured in black clear-bottom 96 well plates and differentiated as described previously [32]. Adipocytes were used for experiments 9-10 days after the onset of differentiation. Cells were incubated for 60 min in serum-free DMEM supplemented with 0.2% BSA and for 30 min in Ringer assay buffer (see above) containing 0.2% BSA, followed by the measurement of background fluorescence at 485 nm excitation and 520 nm emission wavelengths (BMG Fluostar

Optima microtitre plate reader; BMG Labtechnologies, Offenburg, Germany) and the addition of 5 μM $DCFH_2$-DA. Cells were pretreated with H_2O_2, rotenone, 1,10-phenanthroline (PNT), ferric ammonium citrate (FAC), or harman. Before and after the cells were incubated for 15 min at 37°C with DCF-DA, they were extensively washed in order to remove extracellular stimuli and extracellular $DCFH_2$-DA/DCF, respectively. After the final washes, new assay buffer was added to the cells and fluorescence was measured again. The increase in fluorescence between the two measurements was determined and represented the cellular oxidative stress.

Statistics

All data are presented as means ± standard deviation. Experiments were repeated at least three times. For all 96 well plates, two or three wells were used for each condition. Data sets were compared using unpaired two-tailed Student's t-tests (GraphPad Prism). Differences between data sets were considered statistically different when $P<0.05$.

Results

In Fenton chemistry in the absence of cells and proteins, DCF, unlike TBARS, is a reporter for hydroxyl radicals but not for hydrogen peroxide

Using a cell- and protein-free *in vitro* system, we studied the Fenton reaction in the physiological Ringer's saline solution at 37˚C using the ROS-sensitive fluorescent probe 2',7'-dichlorodihydrofluorescein (DCF; Suppl. Fig. S1). A 30 minute co-incubation of H_2O_2 and ferrous iron (Fe^{2+}) dose-dependently increased DCF fluorescence (Fig. 1A, upper left panel). In agreement with data from others, Fe^{2+} oxidized DCF to a minor extent in the absence of H_2O_2 [19]. Interestingly, at none of the concentrations studied, H_2O_2 increased DCF fluorescence in the absence of iron, indicating that in this system, DCF detected hydroxyl radicals but not H_2O_2. The co-incubation of ferrous iron and H_2O_2 resulted in a reduction in the concentrations of both H_2O_2 (Fig. 1A, upper right panel) and ferrous iron (Fig. 1A, lower left panel), and in the generation of ferric iron (Fe^{3+}) (Fig. 1A, lower right panel), providing further evidence for the presence of the Fenton reaction in our system and the generation of hydroxyl radicals.

For the detection of hydroxyl radicals, the measurement of thiobarbituric acid (TBA)-reactive 2-deoxy-D-ribose degradation products is frequently being used. We compared DCF (Fig. 1B) and TBA-reactive substances (TBARS) methods (Fig. 1C). Using the TBARS method, we readily detected hydroxyl radicals (dependent on the concentrations of both H_2O_2 and ferrous iron). However, in the presence of high concentrations of H_2O_2, a significant TBARS signal was also detected in the absence of iron, demonstrating that while this method mostly detected hydroxyl radicals, some reactivity was also seen towards H_2O_2 (Fig. 1C and 1D). In co-incubations of Fe^{2+} and H_2O_2, comparison of Fe^{2+} and H_2O_2 dose-response curves revealed that the DCF and TBARS methods displayed comparable sensitivity towards the detection of hydroxyl radicals (Suppl. Fig. S2A,B). However, variability between triplicate samples was lower for the DCF method (i.e. error bars in Fig. 1B and Suppl. Fig. S2A versus Fig. 1C and Suppl. Fig. S2B), which was likely due to the lower number of handlings in the DCF assay. Another difference between both methods was that, in contrast to the TBARS signal, DCF fluorescence still largely increased between 30 and 120 minutes of incubation (Suppl. Fig. S2C). As expected, H_2O_2/Fe^{2+}-induced DCF fluorescence was inhibited by metal ion chelator EDTA (ethylenediaminetetraacetic acid), by anti-oxidants trolox and buthylhydroxyanisole (BHA) and by hydroxyl scavengers mannitol and harman (Fig. 1E).

The iron/hydrogen peroxide-mediated generation of hydroxyl radicals, as measured by DCF, requires ferrous iron rather than ferric iron - effects of ascorbate

Other *in vitro* systems, not involving DCF, have shown that ascorbate enhances the Fenton reaction by reducing ferric iron (Fe^{3+}) into ferrous iron (Fe^{2+}) [33,34]. To examine the effect of ascorbate on the DCF-mediated detection of Fenton-generated hydroxyl radicals, experiments were performed in which ascorbate was co-incubated with H_2O_2 and either Fe^{2+} or Fe^{3+} (Fig. 2). However, ascorbate can react directly with H_2O_2, which also leads to the generation of hydroxyl radicals [16]. Our studies demonstrated that increases in DCF fluorescence induced by H_2O_2/ascorbate were only detectable after more than 7.5 minutes of incubation while Fe^{2+}/H_2O_2- and Fe^{3+}/H_2O_2/ascorbate-generated

hydroxyl radicals were already detectable after 5 minutes (Suppl. Fig. S3A). Increases in DCF fluorescence due to the ascorbate/H_2O_2-mediated generation of hydroxyl radicals were maximal at 3-10 μM ascorbate, reduced by hydroxyl scavenger mannitol, and accompanied by reductions in H_2O_2 concentrations (Suppl. Fig. S3B-D).

To be able to specifically study the effect of ascorbate on the H_2O_2/iron-mediated generation of hydroxyl radicals, incubation times were set at 7.5 minutes. In contrast to Fe^{2+}, Fe^{3+} did not increase DCF fluorescence in the presence of H_2O_2 within this time frame (Fig 2A). It only increased fluorescence from 40 minutes onwards, which was further enhanced by metal chelator EDTA but not by iron chelator DTPA (Suppl. Fig. S4). While ascorbate did not affect Fe^{2+}/H_2O_2-induced DCF fluorescence in the 7.5 minute incubations, it largely increased DCF fluorescence for the combination of Fe^{3+} and H_2O_2 (Fig. 2A). DCF signal in control incubations with either Fe^{2+}, Fe^{3+}, or H_2O_2 was not increased by ascorbate. We next established ascorbate dose-response curves. In the presence of 10 μM Fe^{2+} and 100 μM H_2O_2, high concentrations of ascorbate reduced DCF fluorescence, likely due to the anti-oxidant action of ascorbate towards hydroxyl radicals and/or H_2O_2 (Fig. 2B, left panel) [35,36]. The combination of 10 μM Fe^{3+} and 100 μM H_2O_2 did not increase DCF fluorescence above background signal unless 3 to 100 μM ascorbate was present (Fig. 2B, right panel). Also here, higher ascorbate concentrations reduced the DCF signal. The intermediate concentrations of ascorbate presumably allowed Fe^{3+} to increase DCF signal via the ascorbate-mediated reduction of Fe^{3+} into Fe^{2+}. To investigate this, 10 μM of either Fe^{2+} or Fe^{3+} was incubated for 7.5 min with various concentrations of ascorbate, followed by the measurement of Fe^{2+} and Fe^{3+} levels (Fig. 2C, upper panels). This confirmed that ascorbate at concentrations higher than 1 μM had indeed converted part of Fe^{3+} into Fe^{2+} (Fig. 2C, upper right panel). When co-incubated with Fe^{2+}, ascorbate fully restored Fe^{2+} levels to 10 μM at the expense of Fe^{3+}, suggesting that it protected Fe^{2+} from auto-oxidation (Fig. 2C, upper left panel).

The addition of H_2O_2 to these incubations demonstrated that, due to the Fenton reaction, all Fe^{2+} had been converted into Fe^{3+} within 7.5 minutes in the absence of ascorbate (Fig. 2C, lower left panel). Ascorbate, from 100 μM onwards, fully restored Fe^{2+} levels. For the combination of Fe^{3+} and H_2O_2, ascorbate at concentrations higher than 100 μM induced the appearance of Fe^{2+} ions, while reducing Fe^{3+} levels, indicating that ascorbate had reduced part of Fe^{3+} to Fe^{2+} (Fig. 2C, lower right panel). At intermediate ascorbate levels (1-100 μM), the small amount of Fe^{2+} that was generated from Fe^{3+} by ascorbate (Fig. 2C, upper right panel) was no longer present if H_2O_2 was added to the incubations (Fig. 2C, lower right panel), due to the rapid Fenton-mediated generation of hydroxyl radicals (Fig. 2B, right panel), leading to the oxidation of Fe^{2+} into Fe^{3+}.

So far, our experiments had failed to demonstrate that ascorbate could increase DCF signal in the presence of H_2O_2 and Fe^{2+} (Fig. 2A and 2B, left panel). This was unexpected, since ascorbate is supposed to recycle Fenton-produced Fe^{3+} back into Fe^{2+} which could then participate in another Fenton reaction ('redox cycling'), further increasing hydroxyl radical levels [3,37]. To investigate this, 10 μM ascorbate and 100 μM H_2O_2 were co-incubated with DCF and various concentrations of either Fe^{2+} or Fe^{3+} (Fig. 2D). This demonstrated that Fe^{2+}/H_2O_2-mediated hydroxyl radical production, as measured by DCF, could indeed be increased by ascorbate, but that this required very low Fe^{2+} levels, between 0.1 and 1 μM, concentrations at which hydroxyl radicals were barely

detectable by DCF in the absence of ascorbate (Fig. 2D, left panel). Similar concentrations were required for maximum pro-oxidative effects of Fe^{3+} (Fig. 2D, right panel).

DCF auto-amplifies its hydroxyl radical-induced fluorescence

Paradoxically, our data had shown that while the Fenton reaction had fully depleted ferrous iron levels within 7.5 minutes of incubation (Fig 2C, lower left panel), DCF signal largely increased between 30 and 120 minutes of incubation (Suppl. Fig. S2C). Measuring DCF fluorescence in time for up to 2 hours demonstrated that it steadily increased in an Fe^{2+}- and H_2O_2-dependent fashion (Fig 3A). Further detailed analyses demonstrated that fluorescence still largely increased after 2 hours of incubation and that at 2 hours of incubation, less than 1% of DCF was oxidized (Suppl. Fig. S5). Remarkably, Fe^{2+}/H_2O_2-induced DCF fluorescence was already significantly increased at the initial measurement (figure insert, 0 minutes; see also Suppl. Fig. S3A). This indicated that Fenton chemistry was quicker than that we could measure using our equipment and that DCF became oxidized by Fe^{2+}/H_2O_2-generated hydroxyl radicals within ~20 seconds at room temperature. In sharp contrast, low level Fe^{2+}-induced DCF oxidation in the absence of H_2O_2 was only measurable after 22 minutes of incubation at 37°C (not shown). In accordance, in the presence of H_2O_2, most of the Fe^{2+} had been instantly transformed into Fe^{3+} (at 0 minutes) and fully converted within 7.5 minutes (Fig. 3B). In the absence of H_2O_2, it took about 2 hours for all Fe^{2+} to oxidize into Fe^{3+}. When replacing Fe^{2+} by Fe^{3+} in these experiments, Fe^{3+} levels remained at 10 μM, both in the absence as well as in the presence of H_2O_2 (data not shown).

To investigate whether the Fenton reaction was still generating hydroxyl radicals after virtually all Fe^{2+} had been converted into Fe^{3+}, the Fenton reaction was initiated with DCF present from the beginning or with DCF added 15 to 60 minutes later on (i.e. when there was no more Fe^{2+}) (Fig. 3C). Then the increase in fluorescence from 60 to 120 minutes was measured. If DCF would not interfere with or participate in any reaction other than its proper reporter reaction, then the amount of newly generated radicals and thus the increase in DCF fluorescence from 60 to 120 minutes would be similar between an incubation in which DCF was added later on ('DCF-2') and its control in which DCF was present from the beginning and buffer was added later on ('DCF-1'), irrespective of differences in fluorescence at 60 minutes. In sharp contrast, our experiments demonstrated that the earlier the DCF was added during the first hour of the incubations, the higher the increase in DCF signal during the second hour (DCF-2 signal in Fig. 3D). This implied that oxidation of DCF during the first hour was required for the increase of its fluorescence during the second hour and thus that oxidized DCF was auto-amplifying its own signal. In addition, in incubations in which DCF was present from the beginning, increases in DCF fluorescence during the second hour were largely inhibited by hydroxyl scavenger mannitol when added at 0 minutes but not at 60 minutes (Fig. 3E). Similar results were obtained when 1.5 mM EDTA was added instead of mannitol (Fig. 3F). In case both DCF and catalase were present at the initiation of the Fenton reaction, H_2O_2 was depleted within 30 minutes, but DCF fluorescence continued to increase steadily up to 120 minutes (Fig. 3G). Of note, the increase in DCF signal during the second hour in the presence of catalase largely exceeded the increase in DCF fluorescence in incubations in which Fe^{2+} but not H_2O_2 was present at the beginning of the incubation (grey line in

Fig. 3G). In the absence of auto-amplification, these increases would have been identical. Together, these data (Fig. 3E-G) demonstrated that during the second hour, oxidized DCF auto-amplified its fluorescence in the absence of Fenton chemistry. DCF auto-amplification appeared to involve a ROS-associated oxidative process since the powerful anti-oxidant dimethylthiourea instantaneously abolished all increases in DCF fluorescence when added at any time after initiation of the Fenton reaction, though 25 μM trolox was only effective at reducing DCF fluorescence when added at the beginning of the Fenton reaction, but not after 60 minutes (not shown). Irrespective of the way DCF auto-amplified its own fluorescence, it did not affect Fe^{2+}, Fe^{3+}, and H_2O_2 levels during the incubations (data not shown).

DCF detects hydrogen peroxide and hydroxyl radicals in the presence of BSA or other proteins

Since proteins are naturally present in biological systems, the effect of model protein bovine serum albumin (BSA) on H_2O_2/hydroxyl radical detection by DCF was investigated. In sharp contrast to incubations without BSA, the presence of 0.2% BSA permitted H_2O_2 to largely increase DCF fluorescence (Fig. 4A). The fluorescence induced by a 30 minute incubation of 5 μM DCF with 100 μM H_2O_2 and 0.2% BSA corresponded to 0.7% of the maximum H_2O_2-induced DCF fluorescence (Suppl. Fig. S6A), demonstrating that the relatively low concentration of DCF was not a rate-limiting factor. Higher concentrations of DCF increased H_2O_2-induced DCF fluorescence without changing this percentage (Suppl. Fig. S6A-C). The BSA-induced increase in DCF fluorescence was not due to an effect of BSA on H_2O_2 levels during the incubations (Fig. 4B). Hydrogen peroxide concentration-dependent increases in DCF fluorescence were analyzed at a low and high concentration of BSA and demonstrated that for both concentrations, H_2O_2 dose-response curves were biphasic and perfectly linear up to 1 μM with a detection limit of 100 nM (Suppl. Fig. S7).

Remarkably, the kinetics of DCF fluorescence in H_2O_2/BSA/DCF incubations were rather logarithmic, in contrast to the kinetics of hydroxyl radical-induced DCF fluorescence in BSA-free incubations which were exponential (Fig. 4C, left panel). The difference in kinetics was even more evident when these data were expressed as increases in fluorescence during 15 minute intervals (Fig. 4C, right panel). Moreover, it demonstrated that the H_2O_2/BSA/DCF reaction took mostly place within the first 60 minutes of incubation. This was confirmed by experiments in which DCF was added directly when H_2O_2 and BSA were combined or 60 minutes later, because in case the DCF was added later, the increase in DCF fluorescence was largely reduced (Fig. 4D). Interestingly, the increase in DCF fluorescence during the second hour was independent of whether DCF was present from the beginning ('DCF-1') or added after 60 minutes ('DCF-2'), providing evidence for the absence of signal auto-amplification in H_2O_2/BSA-induced DCF fluorescence. Absence of auto-amplification was also evident from incubations in which catalase was included (Fig. 4E). Upon catalase-induced depletion of H_2O_2 (at ~30 minutes), further increases in DCF fluorescence in H_2O_2 incubations were strongly reduced and no longer different from increases in control incubations without H_2O_2.

The presence of BSA did not prevent Fenton chemistry and still allowed DCF to react with hydroxyl radicals, since the effect of the combination of Fe^{2+} and H_2O_2 on

DCF was more pronounced than the sum of the effects of the compounds applied separately (Fig. 5A,B). While 1 μM Fe^{2+} and 10 μM H_2O_2 together induced twice the amount of DCF fluorescence compared with the sum of fluorescence induced by H_2O_2 and Fe^{2+} separately (Fig. 5A), the combination of 10 μM Fe^{2+} and 100 μM H_2O_2 induced twelve times more fluorescence (Fig. 5B). Our studies demonstrated that Fe^{2+}/H_2O_2- but not H_2O_2-induced DCF signal in BSA-containing Ringer's solution was sensitive to EDTA, mannitol, and harman, while both signals were reduced by trolox and BHA, confirming that in the presence of BSA, DCF was capable of detecting both H_2O_2 and hydroxyl radicals (Fig. 5C). Surprisingly, the kinetics of hydroxyl radical-induced DCF fluorescence in the presence of BSA resembled the kinetics of H_2O_2/BSA-induced DCF fluorescence and not those of hydroxyl radical-induced fluorescence in the absence of BSA (Fig. 5D). Remarkably, the presence of 0.2% BSA increased DCF fluorescence ~10-fold in 2 hour 10 μM Fe^{2+}/100 μM H_2O_2 incubations, when compared with similar incubations without BSA, but paradoxically reduced maximum hydroxyl radical-induced DCF fluorescence ~3-fold (Suppl. Fig. S8 vs Suppl. Fig. S5). In contrast to incubations without BSA (Fig. 3D), the addition of DCF 60 minutes after combining H_2O_2, Fe^{2+}, and BSA ('DCF-2') did not change the increase in fluorescence during the second hour of incubation, compared with incubations in which DCF was added at the initiation of the Fenton reaction ('DCF-1', Fig. 5E). Also in favor of absence of auto-amplification in hydroxyl radical/BSA-induced DCF fluorescence was that in the presence of BSA, the addition of catalase at the initiation of the Fenton reaction resulted in a depletion of H_2O_2 and an absence of further increases in DCF fluorescence after 30 minutes of incubation (Fig. 5F).

Further investigation demonstrated that BSA gradually enhanced H_2O_2-induced DCF fluorescence up to the maximum concentration of BSA tested (i.e. 1%), while maximum DCF signals for Fe^{2+} and Fe^{2+}/H_2O_2 were obtained at 0.01% BSA, followed by significantly lower DCF signals at higher concentrations of BSA (Fig. 6A). The decrease at higher BSA concentrations could possibly be due to the scavenging of ROS by BSA, affecting the molecular structure of BSA (Suppl. Fig. S9) and resulting in less ROS available for the oxidation of DCF. BSA from different sources all had a positive effect on the detection of H_2O_2 and hydroxyl radicals by DCF (Fig. 6B, left and right panel, respectively and Suppl. Fig. S10). Remarkably, for each batch of BSA, the concentration of BSA that displayed the maximum effect on H_2O_2 signal was different from the concentration that maximally increased hydroxyl radical signal. Moreover, between batches, the concentrations of BSA that induced the highest effects on H_2O_2/hydroxyl radical signals were also distinct, as was the magnitude of the BSA effects. Out of the five batches of BSA tested, the three that had been prepared by heat shock, in particular batch I, had the highest effect on H_2O_2-induced DCF fluorescence (relative to background fluorescence) as compared with the two batches that had been prepared using cold ethanol (Fig. 6B, left panel and Suppl. Fig. S10). Hydroxyl-specific DCF signal was particularly boosted by heat shock BSA batch I at low concentrations and by the two cold ethanol BSA batches at high concentrations (Fig. 6B, right panel and Suppl. Fig. S10).

Of the other proteins tested, purified bovine and rabbit IgG, RNase, as well as recombinant alcohol dehydrogenase (ADH) significantly enhanced relative H_2O_2-induced DCF fluorescence, albeit at different concentrations (Fig. 6C, left panel and Suppl. Fig. S11). In contrast, lysozyme was without effect. Rabbit IgG, RNase and alcohol

dehydrogenase also enhanced relative hydroxyl radical-induced DCF fluorescence, in contrast to bovine IgG and lysozyme, which increased hydroxyl radical-specific (i.e. Fe^{2+}/H_2O_2-dependent) signal as much as DCF signal in Fe^{2+} and control incubations (Fig. 6C, right panel and Suppl. Fig. S11). Taken together, these data suggested that the DCF-enhancing effects were not limited to BSA and that likely most proteins may enhance the sensitivity of DCF for hydrogen peroxide and hydroxyl radicals.

In hydrogen peroxide-treated cells, increases in DCF fluorescence are due to intracellular Fenton reaction-generated hydroxyl radicals

Finally, we investigated whether in living cells DCF could detect hydroxyl radicals and whether DCF would be able to detect H_2O_2 directly, or whether DCF would detect H_2O_2 indirectly, via the H_2O_2- and Fe^{2+}-induced formation of hydroxyl radicals (i.e. Fenton reaction) and the reaction of these radicals with DCF (Fig. 7). To this aim, 3T3-L1 adipocytes were exposed to two distinct forms of oxidative stress: H_2O_2 and the mitochondrial respiratory chain complex I inhibitor rotenone, the latter enhancing mitochondrial superoxide production [1] (Fig. 7A). Most of the experiment (Fig. 7A, phases 2-4), including the incubation of the cells with DCF (phase 4), was performed in the absence of fetal bovine serum (FBS), but in the presence of 0.2% BSA. Exposure of the cells to H_2O_2 increased cellular DCF signal, which was fully abrogated by hydroxyl scavenger harman and by the membrane-permeable iron chelator 1,10-phenanthroline (PNT), but further enhanced by ferric ammonium chloride (FAC) (Fig. 7B). This indicated that the intracellular detection of H_2O_2 by DCF was indirect and mediated by the reaction of DCF with hydroxyl radicals, produced in an H_2O_2- and iron-dependent fashion via the Fenton reaction. In sharp contrast, DCF signal in rotenone-treated cells did not change by treating the cells with either harman or PNT, indicating that rotenone-induced oxidative stress, as measured by DCF, was not mediated by neither H_2O_2 nor hydroxyl radicals (Fig. 7C).

We next investigated whether in cells hydroxyl radical-induced DCF fluorescence was subject to auto-amplification (Fig. 7D-F). To this aim, cells were incubated in the absence or presence of H_2O_2, followed by a 15 minute DCF incubation, extensive washes to remove extracellular DCF, and a 60 minute incubation in the absence of H_2O_2 and DCF during which cellular fluorescence was measured. PNT was added at various time points (Fig. 7D). This demonstrated that H_2O_2 increased DCF fluorescence (Fig. 7E) and that after the removal of extracellular DCF, cellular fluorescence continued to increase (Fig. 7F). PNT abrogated the increases in fluorescence during this time, when included in Ringer from the beginning of the H_2O_2 incubation ('I') and also when added during the DCF incubation ('II'). Thus it only took 15 minutes for PNT to fully suppress further increases in H_2O_2-induced fluorescence. Importantly, when added after the removal of extracellular DCF ('III'), PNT initially slowed down the increase in fluorescence but had no effect on increases in fluorescence signal after 30 minutes (Fig. 7, lower right panel), demonstrating DCF fluorescence auto-amplification. When the same experiment was performed in the absence of BSA, H_2O_2-induced fluorescence remained sensitive to harman and PNT and cellular DCF fluorescence auto-amplification was still evident (Suppl. Fig. S12). Remarkably, absolute DCF fluorscence was largely increased for all conditions. Fluorscence signals of cells incubated with 5 μM DCF in the presence of BSA resembled those of cells incubated with 0.6 μM DCF in the absence of BSA (Suppl.

Fig. S13). However, relative background DCF signal was much lower in cells that had been incubated with BSA (Suppl. Fig. S12 and S13).

Discussion

Here, we have shown that in a cell-free *in vitro* system, fluorophore 2',7' dichlorofluorescin diacetate (abbreviated in the current study as DCF) can be used for the quantitative detection of the oxidative stress induced by the two reactive oxygen species hydroxyl radical ($^{\bullet}OH$) and hydrogen peroxide (H_2O_2). In the absence of BSA/protein, DCF detects hydroxyl radicals but not H_2O_2, while in the presence of BSA/protein, DCF fluorescence is increased by both H_2O_2 and hydroxyl radicals. Taken together, DCF appears to be a very useful tool in systems where one or both of these two ROS species is present. A perfect example is the iron-dependent Fenton reaction, studied here in detail, where both H_2O_2 and hydroxyl radicals are involved. Another example is the iron-independent reaction of H_2O_2 with ascorbate, also studied here, and which, like the Fenton reaction, also results in the generation of hydroxyl radicals, albeit with different kinetics (Suppl. Fig. S3). The current study demonstrates that $DCFH_2$-DA does not need to be hydrolyzed into $DCFH_2$ in advance in order to be used as reporter in cell-free studies for the detection of hydroxyl radicals and H_2O_2 and that $DCFH_2$-DA is converted rapidly enough into $DCFH_2$ for the efficient detection of these two ROS. Spontaneous $DCFH_2$-DA acetate ester hydrolysis [38] is reported to occur at a rate of 20% per hour [39], presumably through auto-oxidation [18]. Since these ester bonds appear to be rather fragile, their hydrolysis rate may well be further enhanced by ROS. Various other chemical entities, including sulfonate, phosphinate, and boronic acid esters, are also sensitive to ROS [40-43]. Since in our study hydroxyl radicals and hydrogen peroxide (with BSA as catalyst) almost instantaneously increased DCF fluorescence, it is likely that $DCFH_2$-DA was rapidly deacetylated into $DCFH_2$, rendering it sensitive to oxidation.

Many of our data confirm previous reports that the hydroxyl radical reacts directly with DCF, increasing its fluorescence. First, in a protein-free system, H_2O_2 and Fe^{2+} alone had no effect on DCF, while together (forming the hydroxyl radical according to the Fenton reaction) they rapidly increased DCF fluorescence. Moreover, in line with the Fenton reaction, H_2O_2/Fe^{2+}-induced DCF fluorescence was accompanied by a decrease in H_2O_2 concentrations and by the oxidation of Fe^{2+} into Fe^{3+}. Second, ascorbate reduced Fe^{3+} into Fe^{2+}, enhancing both Fenton chemistry [3,36] and DCF fluorescence. Third, hydroxyl scavengers mannitol and harman substantially inhibited the H_2O_2/Fe^{2+}-induced DCF signal. Fourth, in accordance with studies in which other hydroxyl radical detection systems were used [36,44], EDTA, but not DTPA, enhanced DCF signal in the presence of Fe^{3+} and H_2O_2, presumably by increasing iron's reduction potential [1], enabling it to be reduced by superoxide [44,45]. Finally, ascorbate is known to react with H_2O_2, independent of the presence of iron ions, leading to the generation of hydroxyl radicals [16]. In agreement, in our system ascorbate together with H_2O_2 increased DCF fluorescence in the absence of iron.

Various methods exist to detect hydroxyl radicals in limited *in vitro* systems (especially used to study Fenton chemistry) as described in *Introduction*. One of the most frequently used methods is the reaction of hydroxyl radicals with 2-deoxy-D-ribose followed by the spectrophotometrical measurement of thiobarbituric acid (TBA)-reactive 2-deoxy-D-ribose degradation products [12,14]. Our experiments with both assays have demonstrated that, in the absence of proteins, in contrast to the DCF method, the TBARS assay also showed reactivity towards higher concentrations of H_2O_2. To our opinion, for

measuring Fenton-generated hydroxyl radicals, the DCF protein-free assay seemed to be more straight-forward and more specific. Moreover, when the Fenton reaction was performed in the presence of BSA, we were still able to measure hydroxyl radicals with the DCF assay but not with the TBARS method, which was likely due to the precipitation of the TBARS signal along with the proteins during sample preparation (not shown).

Our results show that in a cell-free system DCF can detect H_2O_2, but only when BSA/protein is present. H_2O_2 was detected in the presence of BSA from five different sources, bovine and rabbit immunoglobulin, alcohol dehydrogenase, and RNaseA. For lysozyme, only at a high concentration of this protein, H_2O_2 marginally increased absolute DCF fluorescence above background levels. However, when expressed relative to background fluorescence (which also increased with lysozyme), this increase was no longer significant. How BSA/protein potentiates the detection of H_2O_2 by DCF is not clear at present. It does not allow the detection of H_2O_2 through an enhancement of the hydrolysis of $DCFH_2$-DA into $DCFH_2$, since $DCFH_2$, like $DCFH_2$-DA, is not oxidized by H_2O_2 in the absence of BSA [6,19].

At first sight, two of our findings suggested that the H_2O_2-induced DCF fluorescence (in the presence of BSA/protein) was not due to a conversion of H_2O_2 into hydroxyl radicals, which then reacted with DCF. First, the EDTA-mediated chelation of iron and copper, possibly (or perhaps likely) present at trace amounts in BSA preparations [1,46] and in other proteins [47], did not reduce H_2O_2-induced DCF fluorescence. Second, H_2O_2-induced fluorescence was not affected by hydroxyl scavengers harman and mannitol. Nevertheless, we cannot completely exclude the possibility that DCF is capable of detecting H_2O_2 in a BSA/protein-containing solution via the formation of hydroxyl radicals. This may be possible through the presence of trace amounts of iron and/or copper ions attached to the proteins tested. Concentrations varying from 15 to 30 micromol of iron per mmol of commercially available albumin have been described, corresponding to 0.5 to 1 μM of iron in a 0.2% albumin solution [46]. In this case, H_2O_2 would locally (site-specifically) generate hydroxyl radicals through Fenton chemistry (or Fenton-like chemistry in case of copper [1]) in close proximity of the BSA molecule. In addition, it is likely that in a BSA-containing solution, the hydrophobic DCF molecule is bound to BSA as well [48]. This would explain the reduced fluorescence of cells incubated with DCF in the presence of BSA (Suppl. Fig. S12 and S13), since the availability of DCF to the cells might have been limited due to its interaction with BSA. Therefore, in cell-free experiments, hydroxyl radicals generated within the vicinity of a BSA molecule would instantaneously react with BSA-bound DCF, so that hydroxyl scavengers would not be able to trap hydroxyl radicals before their reaction with DCF. The incapability of hydroxyl radical scavengers to quench hydroxyl radicals that are generated locally due to substrate-bound metal ions and which then react with the substrate on the spot has been suggested before for DNA and bacteriophages [1,37,49]. Furthermore, EDTA may not be able to chelate the metal ions involved in these Fenton(-like) reactions as these ions may be bound to BSA rather tightly [1]. Four metal binding sites have been identified within albumin that each bind various metal ions, including copper [26,50,51]. Albumin was also found to bind iron [52]. It contains a specific iron binding site, for which the exact location within albumin has not been established [26] and several additional weaker binding sites, accommodating in total up to eight molecules of iron [52]. The binding of iron to albumin may implicate the

carboxyl group on the side chains of aspartic and glutamic acid residues and the imidazol group of histidine residues, both known to play a general role in the binding of metal ions. It may also implicate tyrosine residues, known for their role in iron binding in transferrin and lactoferrin. Also our study has demonstrated that albumin tightly binds iron. Experiments in which we incubated BSA solutions for 24 hours at 37°C with 1.5 mM EDTA under continuous stirring in order to remove metal ions bound to BSA proved unsuccessful: the 24 hour EDTA incubation did not change the effect of BSA on H_2O_2-induced DCF fluorescence, nor did it reduce the even greater increase in DCF fluorescence when BSA was preincubated for 1 hour with 2 μM Fe^{2+} or Fe^{3+} before the addition of EDTA, demonstrating that BSA tightly binds iron ions that cannot be extracted by chelating agents whatsoever (data not shown). The incapability of EDTA to chelate metal ions that are bound to BSA would also explain why EDTA fully reduced hydroxyl radical-specific (H_2O_2/Fe^{2+}) DCF signal in the absence but not in the presence of BSA (Fig. 1E and 5C; percentage of hydroxyl radical-specific DCF signal (excluding DCF signal from background and from H_2O_2 and Fe^{2+} individually) left with EDTA: 0.1 ± 2.3 vs 17.8 ± 3.6, respectively; P=0.002).

Alternatively, BSA and other proteins may bind and alter the three-dimensional conformation of the hydrophobic DCF molecule, which possibly may render the molecule much more sensitive to oxidative agents. This might even allow H_2O_2, which is much less reactive than the hydroxyl radical, to oxidize DCF and to induce DCF fluorescence. This would also explain why background fluorescence increased in the presence of protein and why hydroxyl radicals increased DCF fluorescence much more in the presence than in the absence of BSA/protein. Nevertheless, why BSA from different sources enhanced relative and absolute H_2O_2- and hydroxyl radical-induced DCF fluorescence at different concentrations and to a different extent is unclear at present. Moreover, the BSA concentration curves for relative (Fig. 6B) and absolute (Fig. 6A and Suppl. Fig. S10) H_2O_2- and hydroxyl radical-induced DCF fluorescence are mostly bell-shaped, implying that the underlying mechanisms are multifactorial and that BSA displays both enhancing and inhibitory effects on either Fenton chemistry or on the detection of hydroxyl radicals by DCF. In addition to the effect of BSA and other proteins on the conformation and sensitivity of DCF and the possible contamination with metal ions, other factors affecting ROS-induced DCF fluorescence may include contaminations with other proteins/peptides, and protein-mediated ROS scavenging (Suppl. Fig. S9) [1,26,46,47,53].

What is remarkable is that the reaction of DCF with H_2O_2/BSA (i.e. increase of fluorescence) was much more efficient shortly after which these three agents were combined than later on (Fig. 4C). Moreover, when DCF was added 60 minutes after the combination of H_2O_2 and BSA, the increase in DCF fluorescence was much reduced (Fig. 4D). This indicated a transient chemical reaction between H_2O_2 and BSA, from which a newly formed molecule was capable of oxidizing DCF. This adds BSA to the current list of catalysts, capable of turning DCF into an H_2O_2-sensitive probe, that includes Fe^{2+}, Cu^{+}, ascorbate, cytochrome c, peroxidases, catalase, and hematin [16,24,49,54-58]. Given that lysozyme increased absolute DCF fluorescence for all conditions without specifically affecting relative H_2O_2- and hydroxyl radical-induced DCF fluorescence, lysozyme happened to be the most inert or neutral of all proteins tested. Therefore, lysozyme may be the most useful protein in case the presence of a protein is required when studying

Fenton chemistry in test tubes using DCF. In contrast, in case DCF is to be used for the ultra-sensitive detection of H_2O_2, then BSA should be included (e.g. BSA-III at a concentration of 0.05%; Suppl. Fig. S10K), since this largely enhances the sensitivity of DCF for H_2O_2. Alternatively, a combination of ferrous iron and BSA could be used (e.g. BSA-I and BSA-III at 0.01 and 0.2%, respectively; Suppl. Fig. S10D and S10L).

We show that in cell cultures DCF does not seem to react directly with H_2O_2, but indirectly via the formation of hydroxyl radicals, since H_2O_2-mediated increases in DCF fluorescence within living cells were abrogated upon iron chelation and by incubation of the cells with hydroxyl radical scavenger harman. Moreover, in accordance with data from others [59], increasing cellular iron levels increased H_2O_2-induced DCF fluorescence. From these data, several conclusions can be drawn. First, within cells hydroxyl radicals are readily detected by DCF. Second, DCF detects H_2O_2 in cells through intracellular Fenton chemistry. Third, in cells that have very low levels of redox-available iron (i.e. iron not bound to ferritin), DCF may not be able to detect H_2O_2. Fourth, H_2O_2 detection in cells by DCF may be facilitated by preincubating the cells with iron. Fifth, H_2O_2 detection in cells by DCF may be enhanced by iron relocation (increasing redox-available iron) and DCF may even report H_2O_2-induced iron relocation rather than H_2O_2/$^{\bullet}$OH-induced DCF oxidation [60]. Sixth, cellular proteins do not sensitise DCF (enough) for the direct detection of H_2O_2 in intact cells (in contrast to BSA and other proteins in cell-free experiments).

Our studies have demonstrated that in a protein-free system, upon oxidation by hydroxyl radicals, DCF auto-amplifies its own fluorescence signal. Previously, DCF auto-amplification has been attributed to the exposure of DCF to excess of light, leading to the subsequent generation of DCF radicals and superoxide [18,61]. In our experiments, DCF auto-amplification was not due to the exposure of DCF to light during our fluorescence measurements since DCF fluorescence did not change when measurement frequencies were decreased or increased (data not shown). Nevertheless, we hypothesize that the DCF auto-amplification in our system may be due to the DCF radical. When DCF is oxidized by a hydroxyl radical, even in the absence of light, the intermediate DCF radical may be formed from the one-electron oxidation of DCF, in between the formation of 2',7'-dichlorofluorescein out of 2',7'-dichlorofluorescin [22,62] (Suppl. Fig. S1). This radical may lead to the generation of another type of radical (for example superoxide [24,62,63]), which somehow propagates DCF oxidation. Such a chain reaction is likely to explain the exponential increase in DCF fluorescence induced by hydroxyl radicals in the absence of BSA. In contrast, in the presence of BSA, the increase in DCF fluorescence induced by either H_2O_2 or hydroxyl radicals was not exponential but logarithmic. Remarkably, in these two cases, there was no auto-amplification. Why hydroxyl radicals lead to DCF fluorescence auto-amplification in the absence of BSA but not in the presence of BSA is unclear at present. Our results have demonstrated that while Fenton chemistry initiated DCF oxidation, it was not involved in the subsequent auto-amplification process since DCF fluorescence auto-amplification was insensitive to hydroxyl scavenger mannitol, metal ion chelator EDTA, and H_2O_2 depletion by catalase. While DCF auto-amplified its fluorescence, it did not participate in Fenton chemistry since DCF did not affect Fe^{2+}, Fe^{3+}, and H_2O_2 concentrations. Of note, the kinetics of the relative increases in Fe^{2+}/H_2O_2-induced DCF signal (compared with basal and Fe^{2+} signals) did not change when DCF concentrations were varied between 0.1 μM (lowest

concentration required for the measurement of hydroxyl radicals) and 10 μM (data not shown), suggesting that hydroxyl radical-induced DCF fluorescence auto-amplification is an intrinsic feature of DCF and not due to the use of high DCF concentrations. This auto-amplification phenomenon is not necessarily a negative aspect of DCF as it may possibly sensitize its detection of ROS. Especially since we have demonstrated DCF fluorescence auto-amplification in cells (incubated in BSA-free as well as in BSA-containing Ringer solution), it may very well be possible that without its auto-amplification, it would be impossible for DCF to detect H_2O_2-induced cellular oxidative stress, and perhaps even oxidative stress induced by other factors as well. DCF fluorescence auto-amplification has previously been described for a cell-free *in vitro* system consisting of DCF, HRP, and peroxynitrite [64]. Here, auto-amplification appeared to be driven by the formation of H_2O_2, which is unlikely to be case in our experiments, since in our study ongoing auto-amplification did not require H_2O_2.

In summary, we demonstrate that DCF is an easy and powerful tool for the detection of both H_2O_2 and hydroxyl radicals in *in vitro* assays. Moreover, the omission of proteins from these assays allows the specific detection of hydroxyl radicals, even if both ROS are present. In this case, DCF auto-amplifies its own fluorescence after its oxidation by hydroxyl radicals. Within cells, despite the presence of proteins, DCF does not detect H_2O_2 directly, but indirectly via the Fenton reaction-mediated conversion of H_2O_2 into hydroxyl radicals, which oxidize DCF.

Abbreviations

BHA, buthylhydroxyanisole; DCF, 2',7'-dichlorofluorescein; DCF-DA, DCF diacetate; DTPA, diethylenetriaminepentaacetic acid; FAC, ferric ammonium citrate; HRP, horse radish peroxidase; OPD, o-phenylenediamine; PNT, 1,10-phenanthroline; ROS, reactive oxygen species; TBA, thiobarbituric acid; TBARS, TBA-reactive substances.

Author Contribution

T.G. performed most of the experiments. F.P., C.D., P.B., and T.G. contributed to data interpretation and manuscript writing. R.G. conceived and designed all experiments, contributed to data interpretation, and wrote the initial draft of the manuscript. All authors reviewed the results and approved the final version of the manuscript.

Acknowledgements

This work was supported by the Institut national de la santé et de la recherche médicale (INSERM), the University of Aix-Marseille (AMU), and the Institut national de recherche pour l'agriculture, l'alimentation et l'environnement (INRAE). We thank Jacek Zielonka (Medical College of Wisconsin, Milwaukee, USA) and Xiuping Chen (Institute of Chinese Medical Sciences, University of Macau, China) for helpful discussions.

Competing Interests

The authors declare that there are no competing interests associated with the manuscript.

References

1 Halliwell, B. and Gutteridge, J. M. (2007) Free radicals in biology and medicine. Oxford University Press

2 Barbusinski, K. (2009) Fenton reaction - controversy concerning the chemistry. Ecol. Chem. Eng. S. **16**, 347-358

3 Hou, X., Huang, X., Ai, Z., Zhao, J. and Zhang, L. (2016) Ascorbic acid/Fe@Fe2O3: A highly efficient combined Fenton reagent to remove organic contaminants. J. Hazard. Mater. **310**, 170-178

4 Klebanoff, S. J., Waltersdorph, A. M., Michel, B. R. and Rosen, H. (1989) Oxygen-based free radical generation by ferrous ions and deferoxamine. J. Biol. Chem. **264**, 19765-19771

5 Gutteridge, J. M., Maidt, L. and Poyer, L. (1990) Superoxide dismutase and Fenton chemistry. Reaction of ferric-EDTA complex and ferric-bipyridyl complex with hydrogen peroxide without the apparent formation of iron(II). Biochem. J. **269**, 169-174

6 Bromme, H. J., Zuhlke, L., Silber, R. E. and Simm, A. (2008) DCFH2 interactions with hydroxyl radicals and other oxidants--influence of organic solvents. Exp. Gerontol. **43**, 638-644

7 Poljsak, B., Gazdag, Z., Jenko-Brinovec, S., Fujs, S., Pesti, M., Belagyi, J., Plesnicar, S. and Raspor, P. (2005) Pro-oxidative vs antioxidative properties of ascorbic acid in chromium(VI)-induced damage: an in vivo and in vitro approach. J. Appl. Toxicol. **25**, 535-548

8 Poljsak, B. and Raspor, P. (2008) The antioxidant and pro-oxidant activity of vitamin C and trolox in vitro: a comparative study. J. Appl. Toxicol. **28**, 183-188

9 Yoon, J. H., Lee, M. S. and Kang, J. H. (2010) Reaction of ferritin with hydrogen peroxide induces lipid peroxidation. BMB Rep. **43**, 219-224

10 Babizhayev, M. A., Seguin, M. C., Gueyne, J., Evstigneeva, R. P., Ageyeva, E. A. and Zheltukhina, G. A. (1994) L-carnosine (beta-alanyl-L-histidine) and carcinine (beta-alanylhistamine) act as natural antioxidants with hydroxyl-radical-scavenging and lipid-peroxidase activities. Biochem. J. **304**, 509-516

11 Aruoma, O. I., Laughton, M. J. and Halliwell, B. (1989) Carnosine, homocarnosine and anserine: could they act as antioxidants in vivo? Biochem. J. **264**, 863-869

12 Hermes-Lima, M., Wang, E. M., Schulman, H. M., Storey, K. B. and Ponka, P. (1994) Deoxyribose degradation catalyzed by Fe(III)-EDTA: kinetic aspects and potential usefulness for submicromolar iron measurements. Mol. Cell. Biochem. **137**, 65-73

13 Kang, J. H. (2010) Protective effects of carnosine and homocarnosine on ferritin and hydrogen peroxide-mediated DNA damage. BMB Rep. **43**, 683-687

14 Herraiz, T. and Galisteo, J. (2015) Hydroxyl radical reactions and the radical scavenging activity of beta-carboline alkaloids. Food Chem. **172**, 640-649

15 Akashi, K., Miyake, C. and Yokota, A. (2001) Citrulline, a novel compatible solute in drought-tolerant wild watermelon leaves, is an efficient hydroxyl radical scavenger. FEBS Lett. **508**, 438-442

16 Nappi, A. J. and Vass, E. (2000) Hydroxyl radical production by ascorbate and hydrogen peroxide. Neurotox. Res. **2**, 343-355

17 Moura, D. J., Richter, M. F., Boeira, J. M., Pegas Henriques, J. A. and Saffi, J. (2007) Antioxidant properties of beta-carboline alkaloids are related to their antimutagenic and antigenotoxic activities. Mutagenesis. **22**, 293-302
18 Chen, X., Zhong, Z., Xu, Z., Chen, L. and Wang, Y. (2010) 2',7'-Dichlorodihydrofluorescein as a fluorescent probe for reactive oxygen species measurement: Forty years of application and controversy. Free Radic. Res. **44**, 587-604
19 Myhre, O., Andersen, J. M., Aarnes, H. and Fonnum, F. (2003) Evaluation of the probes 2',7'-dichlorofluorescin diacetate, luminol, and lucigenin as indicators of reactive species formation. Biochem. Pharmacol. **65**, 1575-1582
20 Wrona, M., Patel, K. and Wardman, P. (2005) Reactivity of 2',7'-dichlorodihydrofluorescein and dihydrorhodamine 123 and their oxidized forms toward carbonate, nitrogen dioxide, and hydroxyl radicals. Free Radic. Biol. Med. **38**, 262-270
21 Brandt, R. and Keston, A. S. (1965) Synthesis of Diacetyldichlorofluorescin: a Stable Reagent for Fluorometric Analysis. Anal. Biochem. **11**, 6-9
22 Kalyanaraman, B., Darley-Usmar, V., Davies, K. J., Dennery, P. A., Forman, H. J., Grisham, M. B., Mann, G. E., Moore, K., Roberts, L. J., 2nd and Ischiropoulos, H. (2012) Measuring reactive oxygen and nitrogen species with fluorescent probes: challenges and limitations. Free Radic. Biol. Med. **52**, 1-6
23 Keller, A., Mohamed, A., Drose, S., Brandt, U., Fleming, I. and Brandes, R. P. (2004) Analysis of dichlorodihydrofluorescein and dihydrocalcein as probes for the detection of intracellular reactive oxygen species. Free Radic. Res. **38**, 1257-1267
24 Wardman, P. (2007) Fluorescent and luminescent probes for measurement of oxidative and nitrosative species in cells and tissues: progress, pitfalls, and prospects. Free Radic. Biol. Med. **43**, 995-1022
25 Jeitner, T. M. (2014) Optimized ferrozine-based assay for dissolved iron. Anal. Biochem. **454**, 36-37
26 Fanali, G., di Masi, A., Trezza, V., Marino, M., Fasano, M. and Ascenzi, P. (2012) Human serum albumin: from bench to bedside. Mol. Aspects Med. **33**, 209-290
27 Colombo, G., Clerici, M., Giustarini, D., Rossi, R., Milzani, A. and Dalle-Donne, I. (2012) Redox albuminomics: oxidized albumin in human diseases. Antioxid. Redox Signal. **17**, 1515-1527
28 Janatova, J., Fuller, J. K. and Hunter, M. J. (1968) The heterogeneity of bovine albumin with respect to sulfhydryl and dimer content. J. Biol. Chem. **243**, 3612-3622
29 Richarme, G., Mihoub, M., Dairou, J., Bui, L. C., Leger, T. and Lamouri, A. (2015) Parkinsonism-associated protein DJ-1/Park7 is a major protein deglycase that repairs methylglyoxal- and glyoxal-glycated cysteine, arginine, and lysine residues. J. Biol. Chem. **290**, 1885-1897
30 Hayes, G. R. and Lockwood, D. H. (1987) Role of insulin receptor phosphorylation in the insulinomimetic effects of hydrogen peroxide. Proc. Natl. Acad. Sci. USA. **84**, 8115-8119
31 Ma, M., Quan, Y., Li, Y., He, X., Xiao, J., Zhan, M., Zhao, W., Xin, Y., Lu, L. and Luo, L. (2018) Bidirectional modulation of insulin action by reactive oxygen species in 3T3L1 adipocytes. Mol. Med. Rep. **18**, 807-814
32 Talantikite, M., Berenguer, M., Gonzalez, T., Alessi, M. C., Poggi, M., Peiretti, F. and Govers, R. (2016) The first intracellular loop of GLUT4 contains a retention motif. J. Cell Sci. **129**, 2273-2284

33 Rietjens, I. M., Boersma, M. G., Haan, L., Spenkelink, B., Awad, H. M., Cnubben, N. H., van Zanden, J. J., Woude, H., Alink, G. M. and Koeman, J. H. (2002) The pro-oxidant chemistry of the natural antioxidants vitamin C, vitamin E, carotenoids and flavonoids. Environ. Toxicol. Pharmacol. **11**, 321-333
34 Duarte, T. L. and Jones, G. D. (2007) Vitamin C modulation of H2O2-induced damage and iron homeostasis in human cells. Free Radic. Biol. Med. **43**, 1165-1175
35 Karkonen, A. and Fry, S. C. (2006) Effect of ascorbate and its oxidation products on H2O2 production in cell-suspension cultures of Picea abies and in the absence of cells. J. Exp. Bot. **57**, 1633-1644
36 Buettner, G. R. and Jurkiewicz, B. A. (1996) Catalytic metals, ascorbate and free radicals: combinations to avoid. Radiat. Res. **145**, 532-541
37 Samuni, A., Aronovitch, J., Godinger, D., Chevion, M. and Czapski, G. (1983) On the cytotoxicity of vitamin C and metal ions. A site-specific Fenton mechanism. Eur. J. Biochem. **137**, 119-124
38 Kalinich, J. F., Ramakrishnan, N. and McClain, D. E. (1997) The antioxidant Trolox enhances the oxidation of 2',7'-dichlorofluorescin to 2',7'-dichlorofluorescein. Free Rad. Res. **26**, 37-47
39 Royall, J. A. and Ischiropoulos, H. (1993) Evaluation of 2',7'-dichlorofluorescin and dihydrorhodamine 123 as fluorescent probes for intracellular H2O2 in cultured endothelial cells. Arch. Biochem. Biophys. **302**, 348-355
40 Xu, K., Liu, X. and Tang, B. (2007) A phosphinate-based red fluorescent probe for imaging the superoxide radical anion generated by RAW264.7 macrophages. Chem. Bio. Chem. **8**, 453-458
41 Daniel, K. B., Major Jourden, J. L., Negoescu, K. E. and Cohen, S. M. (2011) Activation of sulfonate ester based matrix metalloproteinase proinhibitors by hydrogen peroxide. J. Biol. Inorg. Chem. **16**, 313-323
42 Hu, J. J., Wong, N., Ye, S., Chen, X., Lu, M., Zhao, A. Q., HGuo, Y., Ma, A. C., Leung, A. Y. S., J. and Yang, D. (2015) Fluorescent Probe HKSOX-1 for Imaging and Detection of Endogenous Superoxide in Live Cells and In Vivo. J. Am. Chem. Soc. **137**, 6837-6843
43 Cadahia, J. P., Previtali, V., Troelsen, N. S. and Clausen, M. H. (2019) Prodrug strategies for targeted therapy triggered by reactive oxygen species. Med. Chem. Commun. **10**, 1531-1549
44 Sutton, H. C. (1985) Efficiency of chelated iron compounds as catalysts for the Haber-Weiss reaction. J Free Radic. Biol. Med. **1**, 195-202
45 Gutteridge, J. M. (1990) Superoxide-dependent formation of hydroxyl radicals from ferric-complexes and hydrogen peroxide: an evaluation of fourteen iron chelators. Free Radic. Res. Commun. **9**, 119-125
46 Quinlan, G. J., Coudray, C., Hubbard, A. and Gutteridge, J. M. (1992) Vanadium and copper in clinical solutions of albumin and their potential to damage protein structure. J. Pharm. Sci. **81**, 611-614
47 Wang, W., Ignatius, A. A. and Thakkar, S. V. (2014) Impact of residual impurities and contaminants on protein stability. J. Pharm. Sci. **103**, 1315-1330
48 Subramaniam, R., Fan, X. J., Scivittaro, V., Yang, J., Ha, C. E., Petersen, C. E., Surewicz, W. K., Bhagavan, N. V., Weiss, M. F. and Monnier, V. M. (2002) Cellular

oxidant stress and advanced glycation endproducts of albumin: caveats of the dichlorofluorescein assay. Arch. Biochem. Biophys. **400**, 15-25
49 Sutton, H. C. and Winterbourn, C. C. (1989) On the participation of higher oxidation states of iron and copper in Fenton reactions. Free Radic. Biol. Med. **6**, 53-60
50 Blindauer, C. A., Khazaipoul, S., Yu, R. and Stewart, A. J. (2016) Fatty Acid-Mediated Inhibition of Metal Binding to the Multi-Metal Site on Serum Albumin: Implications for Cardiovascular Disease. Curr. Top. Med. Chem. **16**, 3021-3032
51 Bal, W., Sokolowska, M., Kurowska, E. and Faller, P. (2013) Binding of transition metal ions to albumin: sites, affinities and rates. Biochimb Biophysb Acta. **1830**, 5444-5455
52 Loban, A., Kime, R. and Powers, H. (1997) Iron-binding antioxidant potential of plasma albumin. Clin. Sci. **93**, 445-451
53 Niedzialkowska, E., Gasiorowska, O., Handing, K. B., Majorek, K. A., Porebski, P. J., Shabalin, I. G., Zasadzinska, E., Cymborowski, M. and Minor, W. (2016) Protein purification and crystallization artifacts: The tale usually not told. Protein Sci. **25**, 720-733
54 Hempel, S. L., Buettner, G. R., O'Malley, Y. Q., Wessels, D. A. and Flaherty, D. M. (1999) Dihydrofluorescein diacetate is superior for detecting intracellular oxidants: comparison with 2',7'-dichlorodihydrofluorescein diacetate, 5(and 6)-carboxy-2',7'-dichlorodihydrofluorescein diacetate, and dihydrorhodamine 123. Free Radic. Biol. Med. **27**, 146-159
55 Burkitt, M. J. and Wardman, P. (2001) Cytochrome C is a potent catalyst of dichlorofluorescin oxidation: implications for the role of reactive oxygen species in apoptosis. Biochem. Biophys. Res. Commun. **282**, 329-333
56 Burkitt, M., Jones, C., Lawrence, A. and Wardman, P. (2004) Activation of cytochrome c to a peroxidase compound I-type intermediate by H2O2: relevance to redox signalling in apoptosis. Biochem. Soc. Symp. **71**, 97-106
57 Keston, A. S. and Brandt, R. (1965) The Fluorometric Analysis of Ultramicro Quantities of Hydrogen Peroxide. Anal. Biochem. **11**, 1-5
58 LeBel, C. P., Ischiropoulos, H. and Bondy, S. C. (1992) Evaluation of the probe 2',7'-dichlorofluorescin as an indicator of reactive oxygen species formation and oxidative stress. Chem. Res. Toxicol. **5**, 227-231
59 Tampo, Y., Kotamraju, S., Chitambar, C. R., Kalivendi, S. V., Keszler, A., Joseph, J. and Kalyanaraman, B. (2003) Oxidative stress-induced iron signaling is responsible for peroxide-dependent oxidation of dichlorodihydrofluorescein in endothelial cells: role of transferrin receptor-dependent iron uptake in apoptosis. Circ. Res. **92**, 56-63
60 Karlsson, M., Kurz, T., Brunk, U. T., Nilsson, S. E. and Frennesson, C. I. (2010) What does the commonly used DCF test for oxidative stress really show? Biochem. J. **428**, 183-190
61 Marchesi, E., Rota, C., Fann, Y. C., Chignell, C. F. and Mason, R. P. (1999) Photoreduction of the fluorescent dye 2'-7'-dichlorofluorescein: a spin trapping and direct electron spin resonance study with implications for oxidative stress measurements. Free Radic. Biol. Med. **26**, 148-161
62 Rota, C., Chignell, C. F. and Mason, R. P. (1999) Evidence for free radical formation during the oxidation of 2'-7'-dichlorofluorescin to the fluorescent dye 2'-7'-

dichlorofluorescein by horseradish peroxidase: possible implications for oxidative stress measurements. Free Radic. Biol. Med. **27**, 873-881
63 Wrona, M. and Wardman, P. (2006) Properties of the radical intermediate obtained on oxidation of 2',7'-dichlorodihydrofluorescein, a probe for oxidative stress. Free Radic. Biol. Med. **41**, 657-667
64 Bonini, M. G., Rota, C., Tomasi, A. and Mason, R. P. (2006) The oxidation of 2',7'-dichlorofluorescin to reactive oxygen species: a self-fulfilling prophesy? Free Radic. Biol. Med. **40**, 968-975

Legends

Figure 1. In a cell- and protein-free Fenton reaction, DCF is a reporter for hydroxyl radicals but not for hydrogen peroxide. (**A**) DCF (5 μM) was incubated for 30 min at 37ºC with various concentrations of H_2O_2 and ferrous iron (Fe^{2+}). The relative iron- and H_2O_2-dependent oxidation potential was calculated from the increase in DCF fluorescence (A, upper left panel). At the end of the incubation, concentrations of H_2O_2 (A, upper right panel), Fe^{2+} (A, lower left panel), and Fe^{3+} (A, lower right panel) were measured. Remaining H_2O_2 levels were expressed as percentage of H_2O_2 levels after 30 min in the absence of Fe^{2+}. (**B,C,D**) H_2O_2- and ferrous iron-induced oxidation was analyzed using DCF fluorescence (B) and by measuring thiobarbituric acid (TBA)-reactive degradation products of 2-deoxy-D-ribose (C). Graph D shows selected data from (B) and (C): H_2O_2-dependent DCF and TBARS signals in the absence of ferrous iron, expressed as percentage of maximum signals in B and C. (**E**) DCF was incubated for 30 min at 37ºC in the absence or presence of 100 μM H_2O_2, 10 μM ferrous iron, 1.5 mM EDTA, 25 μM trolox, 200 μM butylhydroxyanisol (BHA), 100 mM mannitol, and 2 mM harman as indicated. Note that higher concentrations of EDTA, trolox, BHA, mannitol, and harman did not further reduce DCF fluorescence. *, $P<0.05$; **, $P<0.01$, ***, $P<0.001$, compared with incubations without ferrous iron (A, top right panel), compared with incubations in the absence of H_2O_2 (A, bottom panels and D), or compared with identical control incubations ('ctrl', E).

Figure 2. Iron/H_2O_2-induced DCF fluorescence in a cell- and protein-free Fenton reaction requires ferrous but not ferric iron. Reactions were performed at 37°C and lasted 7.5 min. (**A**) DCF was incubated in the absence or presence of 100 μM H_2O_2, 10 μM ascorbate, and 10 μM of ferrous or ferric iron. (**B**) Various concentrations of ascorbate were incubated with 100 μM H_2O_2 and 10 μM of either ferrous (left panel) or ferric iron (right panel). Incubations without iron were included as controls. (**C**) Various concentrations of ascorbate were incubated with 10 μM of either ferrous (left panels) or ferric iron (right panels) in the absence (upper panels) or presence of 100 μM H_2O_2 (lower panels). Concentrations of ferrous and ferric iron at the end of the incubations were determined. (**D**) Various concentrations of ferrous (left panel) and ferric iron (right panel) were incubated with DCF and 100 μM H_2O_2 in the absence or presence of 10 μM ascorbate. Increases in DCF fluorescence were determined. *, $P<0.05$; **, $P<0.01$; ***, $P<0.001$, compared with incubations without ascorbate; ns, non-significant.

Figure 3. Hydroxyl radicals induce auto-amplification of DCF fluorescence. (**A**) Ferrous iron was incubated with H_2O_2 and DCF as indicated. Fluorescence was measured every 7.5 min. Insert shows fluorescence for the first 7.5 minutes. (**B**) In parallel incubations, Fe^{2+} and Fe^{3+} levels were measured after 0, 7.5, 15, 30, 60, and 120 min. (**C**) Schematic layout of the experiment in which DCF was present at the initiation of the Fenton reaction ('DCF-1') or added later on ('DCF-2'). DCF-2 incubations received DCF 0, 15, 30, or 60 min after initiation of the reaction, while DCF-1 incubations received the same volume of buffer. Note that for each DCF-1/DCF-2 couple, the only difference was the presence of 5 μM DCF during the first 15, 30, or 60 min of incubation. After the additions at these time points, DCF concentration was 5 μM for both. Increases in

fluorescence from 60 to 120 min after initiation of the Fenton reaction were measured. (**D**) Incubations in the absence or presence of 10 μM Fe^{2+} and 100 μM H_2O_2 were performed as described under C. Each panel displays the increases in fluorescence of the incubations that received either buffer (DCF-1) or DCF (DCF-2) at each indicated time point. Note that fluorescence of 0 μM Fe^{2+}/0 μM H_2O_2 and 0 μM Fe^{2+}/100 μM H_2O_2 incubations increased to maximum 1.0 A.U. (not shown). (**E**) Incubations were similar to those of C and D, except that for all incubations DCF was present from the beginning and that 100 mM mannitol (or buffer as control) was added instead of DCF. Fluorescence of 0 μM Fe^{2+}/0 μM H_2O_2 and 0 μM Fe^{2+}/100 μM H_2O_2 incubations increased to maximum 2.0 A.U. and addition of mannitol at 15 min instead of 60 min resulted in an intermediate effect (data not shown). (**F**) Incubations were similar to those of E, except that 1.5 mM EDTA was added instead of mannitol. (**G**) DCF was incubated with 10 μM Fe^{2+} and 100 μM H_2O_2 in the absence (triangles) or presence of 1 U/ml catalase (squares). DCF fluorescence (closed symbols) and H_2O_2 levels (open symbols) were measured. Grey line depicts DCF fluorescence for 10 μM Fe^{2+} without H_2O_2 within the same experiment. *, $P<0.05$; **, $P<0.01$; ***, $P<0.001$, vs ctrl (A), DCF-1 vs DCF-2 (D), buffer vs mannitol/EDTA (E,F), or DCF in absence vs presence of catalase (G).

Figure 4. In the presence of BSA, hydrogen peroxide increases DCF fluorescence. (**A**) DCF was incubated for 30 min with various concentrations of H_2O_2 in the absence or presence of 0.2% BSA. Increases in DCF fluorescence were measured and expressed as the amount of fluorescence above background fluorescence at 0 μM H_2O_2. Insert is a close-up of the bottom part of the panel and demonstrates that in the absence of BSA, H_2O_2 does not increase DCF fluorescence. (**B**) Various concentrations of H_2O_2 were incubated for 15 min at 37ºC with or without 0.2% BSA in the absence of DCF. Subsequently, H_2O_2 concentrations were determined using calibration curves that were also prepared with or without BSA. Of note, these calibration curves were virtually identical. (**C**) DCF was incubated for 120 min with the indicated concentrations of H_2O_2 in the presence of 0.2% BSA. Fluorescence was measured every 15 min (left panel), increases in fluorescence between measurements were calculated (right panel), and both were expressed as percentage of fluorescence at 120 min in the presence of 100 μM H_2O_2. Grey lines and symbols demonstrate kinetics of DCF fluorescence for 10 μM Fe^{2+}/100 μM H_2O_2 in the absence of BSA. (**D**) H_2O_2 (100 μM) was incubated with 0.2% BSA. DCF was present from the beginning ('DCF-1') or added after 1 hr ('DCF-2'), similarly as in Fig. 3C, and fluorescence was measured. The dotted line corresponds to the DCF signal after 60 min of 'DCF-1' and depicts what was expected for 'DCF-2' at 120 min if any reaction between H_2O_2, BSA and/or DCF was dependent on the presence of all three components. (**E**) DCF was incubated with 0.2% BSA in the absence or presence of 100 μM H_2O_2 and 1 U/ml catalase and DCF fluorescence was measured at 7.5 min intervals (upper panel). For the 100 μM H_2O_2 incubations, the remaining H_2O_2 levels were determined as well (lower panel). *$P<0.05$; **$P<0.01$; ***$P<0.001$, vs background DCF fluorescence at 0 μM H_2O_2 (A), or DCF in absence vs presence of catalase (E).

Figure 5. In the presence of BSA, DCF is a dual reporter for H_2O_2 and the iron/H_2O_2-induced generation of hydroxyl radicals. (**A,B**) DCF was incubated with 0.2% BSA in the absence or presence of either 1 μM ferrous iron and 10 μM H_2O_2 (A) or

10 μM ferrous iron and 100 μM H_2O_2 (B). Fluorescence was measured at different time points. Similar fluorescence units are depicted for panels A and B. Insert in panel B shows the same graph but with a continuous y-axis, better visualizing relative differences between the four curves. (**C**) DCF was incubated for 30 min at 37ºC in the absence or presence of 100 μM H_2O_2, 10 μM ferrous iron, 1.5 mM EDTA, 25 μM trolox, 200 μM buthylhydroxyanisol (BHA), 100 mM mannitol, and 2 mM harman as indicated. Increases in DCF fluorescence were measured. Higher concentrations of EDTA, trolox, BHA, mannitol, and harman did not further reduce DCF fluorescence. (**D**) DCF was incubated with 10 μM Fe^{2+} and 100 μM H_2O_2 in the absence or presence of 0.2% BSA. Fluorescence was measured every 15 min and increases in fluorescence between measurements were expressed as percentage of fluorescence at 120 min (as in right panel of Fig. 4C). Of note, increases in fluorescence for Fe^{2+} and H_2O_2 individually were < 1%. (**E**) Fe^{2+} and H_2O_2, at 10 and 100 μM, respectively, were incubated in the presence of 0.2% BSA. DCF was present at the initiation of the Fenton reaction ('DCF-1') or added 0 or 60 min after combining H_2O_2 and Fe^{2+} ('DCF-2'), similarly as in Fig. 3C. Increases in DCF fluorescence were measured from 60 to 120 min. (**F**) DCF was incubated with 10 μM Fe^{2+} and 100 μM H_2O_2 in the absence (triangles) or presence of 1 U/ml catalase (squares). DCF fluorescence (solid symbols) and H_2O_2 levels (open symbols) were measured. Grey line depicts DCF fluorescence for 10 μM Fe^{2+} without H_2O_2 within the same experiment *, $P<0.05$; **, $P<0.01$, ***, $P<0.001$, vs identical control incubations (C), DCF-1 vs DCF-2 (E), or DCF in absence vs presence of catalase (F).

Figure 6. Dose-dependent effects of BSA and other proteins on hydrogen peroxide- and hydroxyl radical-induced DCF fluorescence. (**A**) DCF was incubated for 30 min in the absence or presence of 10 μM H_2O_2, 1 μM ferrous iron, and various concentrations of BSA. Insert is a close-up of the bottom left part of the panel, showing DCF signals in the absence of BSA (**B**) BSA from different sources (see *Materials and Methods*) was added, at various concentrations, to 10 μM H_2O_2 and/or 1 μM ferrous iron. H_2O_2-induced DCF fluorescence (left panel) was expressed as the increase in fluorescence due to H_2O_2 (in the absence of iron), relative to background DCF fluorescence (in the absence of H_2O_2 and Fe^{2+}). Hydroxyl radical-induced fluorescence (right panel) was expressed as the difference in DCF fluorescence between H_2O_2-specific signals in the presence and absence of iron, relative to background DCF fluorescence. Filled symbols correspond to BSA prepared by heat shock, while open symbols correspond to BSA prepared using cold ethanol (**C**) Various concentrations of the indicated proteins were added to 10 μM H_2O_2 and/or 1 μM ferrous iron. H_2O_2- (left panel) and hydroxyl-specific DCF signal (right panel) was expressed as in (B). For each of the proteins tested, the different concentrations (including a control without protein) were analyzed on the same 96 well plate. *, $P<0.05$; **, $P<0.01$, ***, $P<0.001$, compared with identical incubations without protein.

Figure 7. Within cells, hydrogen peroxide indirectly increases DCF fluorescence via the generation of hydroxyl radicals, which is not accompanied by DCF fluorescence auto-amplification. (**A**) 3T3-L1 adipocytes were incubated at 37°C according to the depicted schematic diagram and underwent four distinct phases: (1) long-term 23 h incubation, (2) 1 h serum (FBS) starvation, (3) 30 min short stimulus incubation, (4) 15

min DCF incubation. Fluorescence was measured before and after DCF incubation (after cell washes). During phases 2-4, 0.2% BSA was present but no serum. Cells were incubated during the indicated phases with combinations of 150 μg/ml FAC, 10 μM PNT, 500 μM harman, 100 μg/ml rotenone, and 250 μM H_2O_2 and were extensively washed at various time points (arrows). (**B**) Cells were incubated with or without H_2O_2 in the absence or presence of harman, PNT, and FAC. (**C**) Cells were incubated with or without rotenone in the absence or presence of harman, PNT, and FAC. (**D**) Serum-starved adipocytes were incubated for 90 min in Ringer/BSA that contained 500 μM H_2O_2 during the first 15 min and DCF for the next 15 min. Cells were washed before and after the DCF incubation. Cellular fluorescence was measured before the addition of DCF ('a'), after the washes that followed the DCF incubation ('b') and during 60 min after the removal of DCF ('c'). PNT (10 μM) or vehicle (DMSO) was included from the beginning of the H_2O_2 incubation ('I'), from the incubation of the cells with DCF ('II') or after the removal of DCF ('III'). (**E**) DCF fluorescence measurements at points 'a' and 'b'. (**F**) Fluorescence was measured at 6 min intervals during period 'c', with PNT added at time points I, II, or III, and expressed as percentage of H_2O_2-specific signal in 'b', indicated in (E) as '100%' (upper panels). Increases in fluorescence between measurements were calculated and expressed as percentage of H_2O_2-specific signal in 'b' (lower panels). *, $P<0.05$; **, $P<0.01$; ***, $P<0.001$; n.s., non-significant. Similar fluorescence units are depicted for panels B and C.

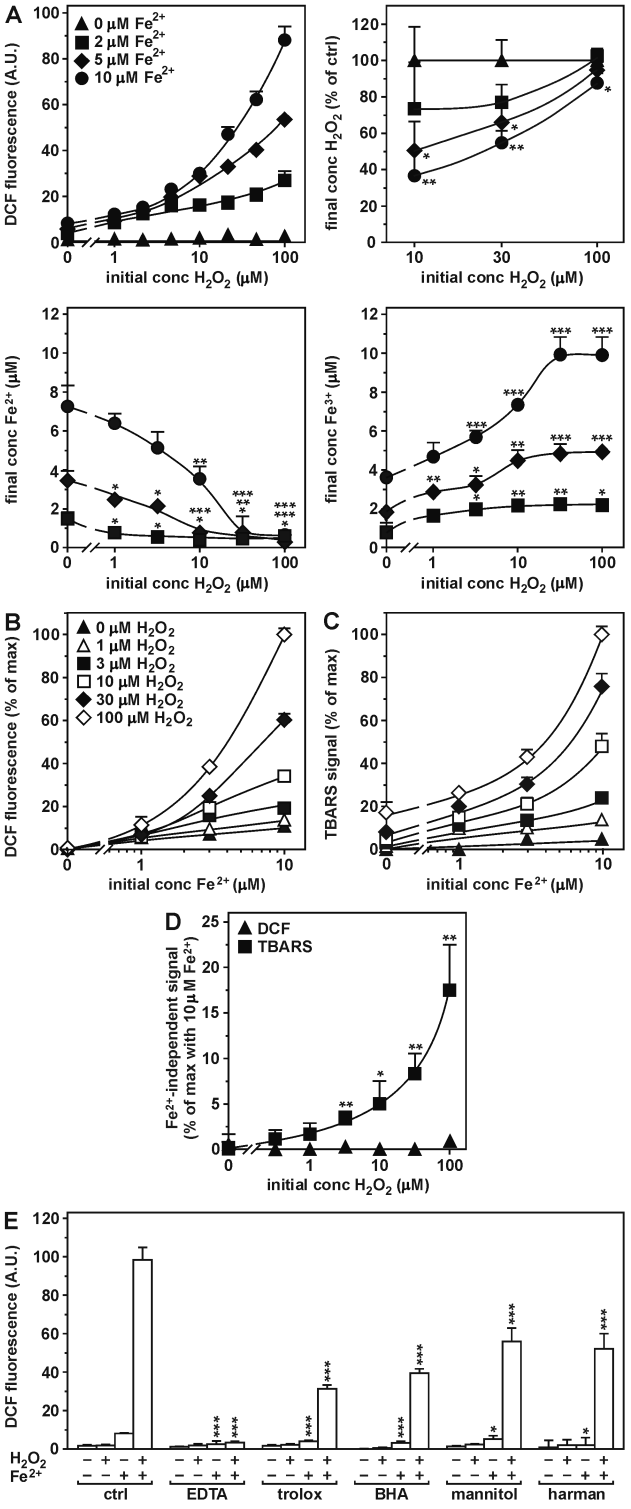
A
0 μM Fe2+
2 μM Fe2+
5 μM Fe2+
10 μM Fe2+
DCF fluorescence (A.U.)
initial conc H2O2 (μM)
final conc H2O2 (% of ctrl)
final conc Fe2+ (μM)
final conc Fe3+ (μM)
B
0 μM H2O2
1 μM H2O2
3 μM H2O2
10 μM H2O2
30 μM H2O2
100 μM H2O2
DCF fluorescence (% of max)
initial conc Fe2+ (μM)
C
TBARS signal (% of max)
D
DCF
TBARS
Fe2+-independent signal (% of max with 10 μM Fe2+)
E
DCF fluorescence (A.U.)
H2O2
Fe2+
ctrl
EDTA
trolox
BHA
mannitol
harman

Fig. 1

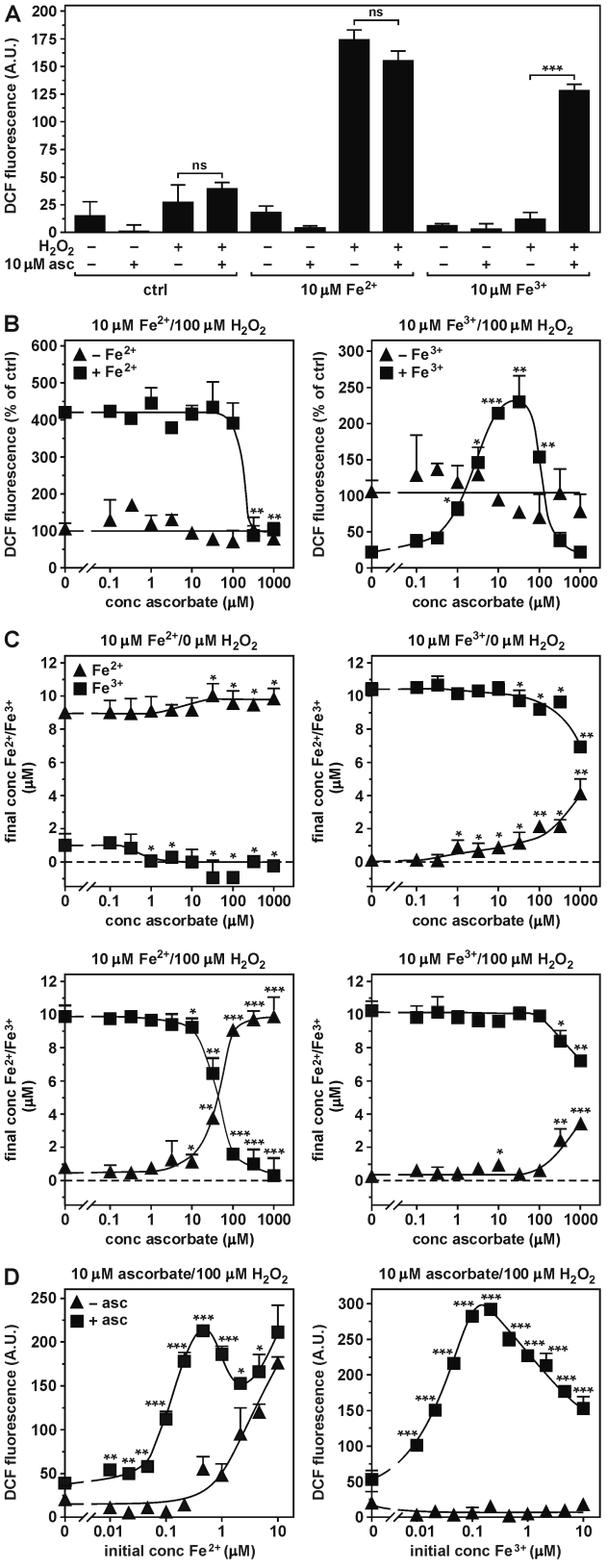
A
DCF fluorescence (A.U.)
ns
ns
***
H2O2
10 µM asc
ctrl
10 µM Fe2+
10 µM Fe3+
B
10 µM Fe2+/100 µM H2O2
10 µM Fe3+/100 µM H2O2
– Fe2+
+ Fe2+
– Fe3+
+ Fe3+
DCF fluorescence (% of ctrl)
conc ascorbate (µM)
C
10 µM Fe2+/0 µM H2O2
10 µM Fe3+/0 µM H2O2
10 µM Fe2+/100 µM H2O2
10 µM Fe3+/100 µM H2O2
Fe2+
Fe3+
final conc Fe2+/Fe3+ (µM)
conc ascorbate (µM)
D
10 µM ascorbate/100 µM H2O2
10 µM ascorbate/100 µM H2O2
– asc
+ asc
DCF fluorescence (A.U.)
initial conc Fe2+ (µM)
initial conc Fe3+ (µM)

Fig. 2

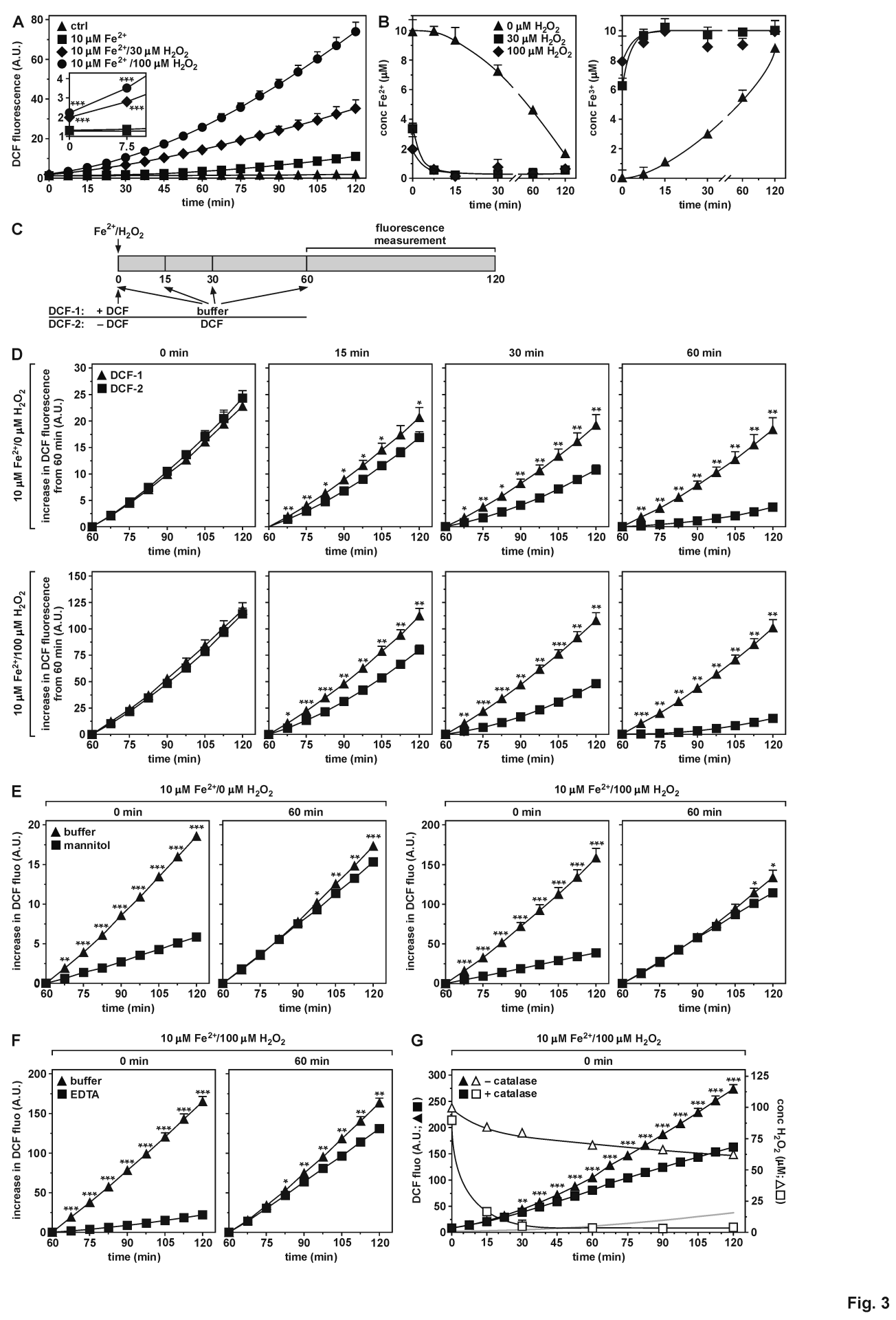
A
ctrl
10 µM Fe2+
10 µM Fe2+/30 µM H2O2
10 µM Fe2+ /100 µM H2O2
DCF fluorescence (A.U.)
time (min)
B
0 µM H2O2
30 µM H2O2
100 µM H2O2
conc Fe2+ (µM)
conc Fe3+ (µM)
time (min)
C
Fe2+/H2O2
fluorescence measurement
DCF-1: + DCF
DCF-2: – DCF
buffer
DCF
D
0 min
15 min
30 min
60 min
DCF-1
DCF-2
10 µM Fe2+/0 µM H2O2
10 µM Fe2+/100 µM H2O2
increase in DCF fluorescence from 60 min (A.U.)
time (min)
E
10 µM Fe2+/0 µM H2O2
10 µM Fe2+/100 µM H2O2
buffer
mannitol
increase in DCF fluo (A.U.)
F
buffer
EDTA
G
– catalase
+ catalase
DCF fluo (A.U.; ▲■)
conc H2O2 (µM; △□)

Fig. 3

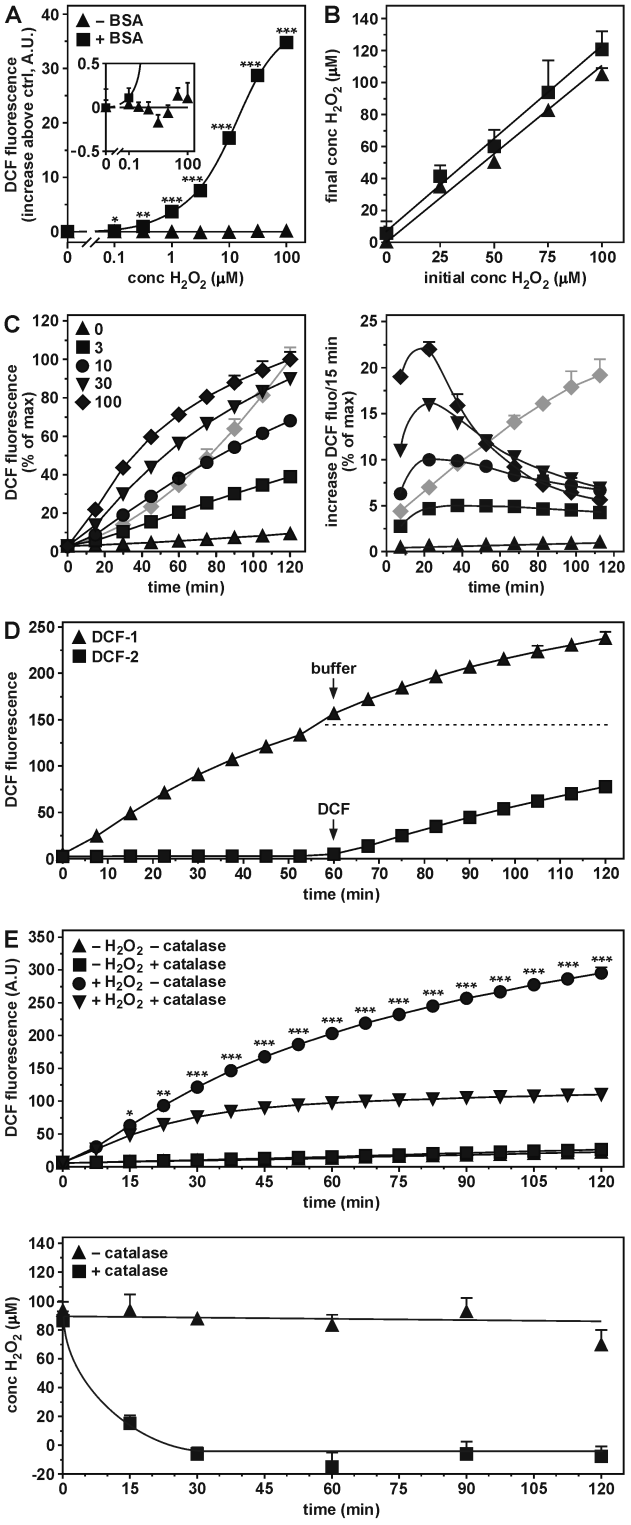
A
– BSA
+ BSA
DCF fluorescence (increase above ctrl, A.U.)
conc H_2O_2 (μM)
B
final conc H_2O_2 (μM)
initial conc H_2O_2 (μM)
C
0
3
10
30
100
DCF fluorescence (% of max)
time (min)
increase DCF fluo/15 min (% of max)
time (min)
D
DCF-1
DCF-2
buffer
DCF
DCF fluorescence
time (min)
E
– H_2O_2 – catalase
– H_2O_2 + catalase
+ H_2O_2 – catalase
+ H_2O_2 + catalase
DCF fluorescence (A.U)
time (min)
– catalase
+ catalase
conc H_2O_2 (μM)
time (min)

Fig. 4

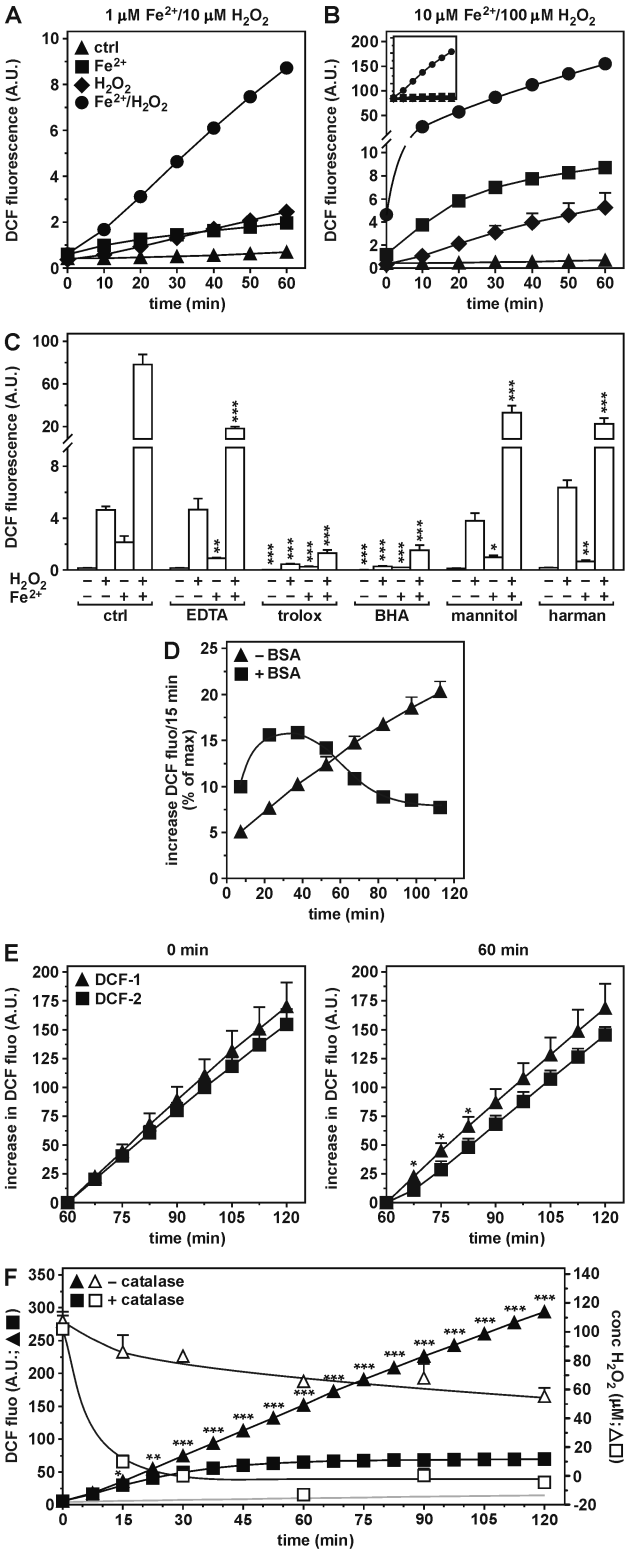
A
1 μM Fe2+/10 μM H2O2
ctrl
Fe2+
H2O2
Fe2+/H2O2
DCF fluorescence (A.U.)
time (min)
B
10 μM Fe2+/100 μM H2O2
DCF fluorescence (A.U.)
time (min)
C
DCF fluorescence (A.U.)
H2O2
Fe2+
ctrl
EDTA
trolox
BHA
mannitol
harman
D
– BSA
+ BSA
increase DCF fluo/15 min (% of max)
time (min)
E
0 min
60 min
DCF-1
DCF-2
increase in DCF fluo (A.U.)
time (min)
F
– catalase
+ catalase
DCF fluo (A.U.; ▲■)
conc H2O2 (μM; △□)
time (min)

Fig. 5

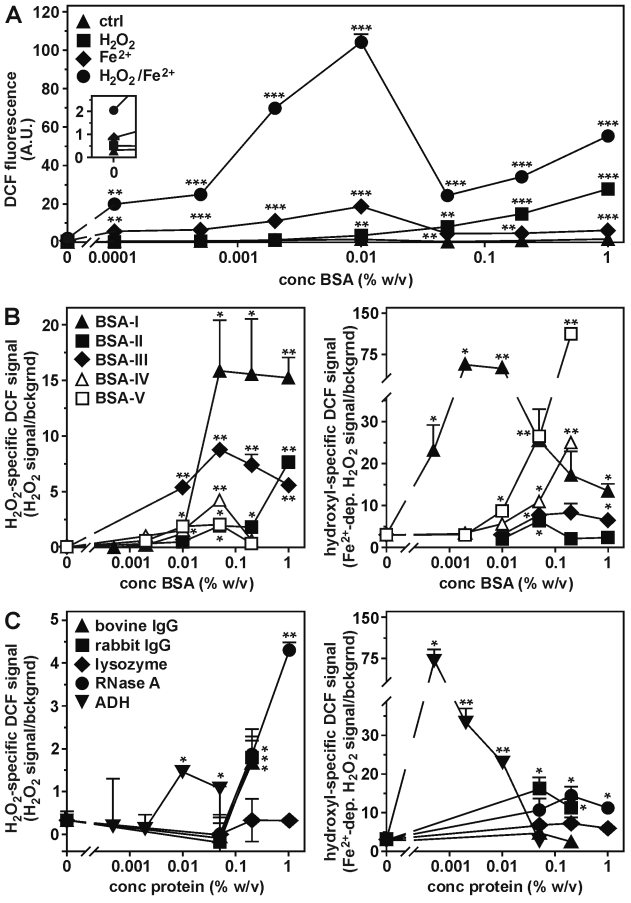
A
ctrl
H2O2
Fe2+
H2O2/Fe2+
DCF fluorescence (A.U.)
conc BSA (% w/v)
B
BSA-I
BSA-II
BSA-III
BSA-IV
BSA-V
H2O2-specific DCF signal (H2O2 signal/bckgrnd)
hydroxyl-specific DCF signal (Fe2+-dep. H2O2 signal/bckgrnd)
conc BSA (% w/v)
C
bovine IgG
rabbit IgG
lysozyme
RNase A
ADH
H2O2-specific DCF signal (H2O2 signal/bckgrnd)
hydroxyl-specific DCF signal (Fe2+-dep. H2O2 signal/bckgrnd)
conc protein (% w/v)

Fig. 6

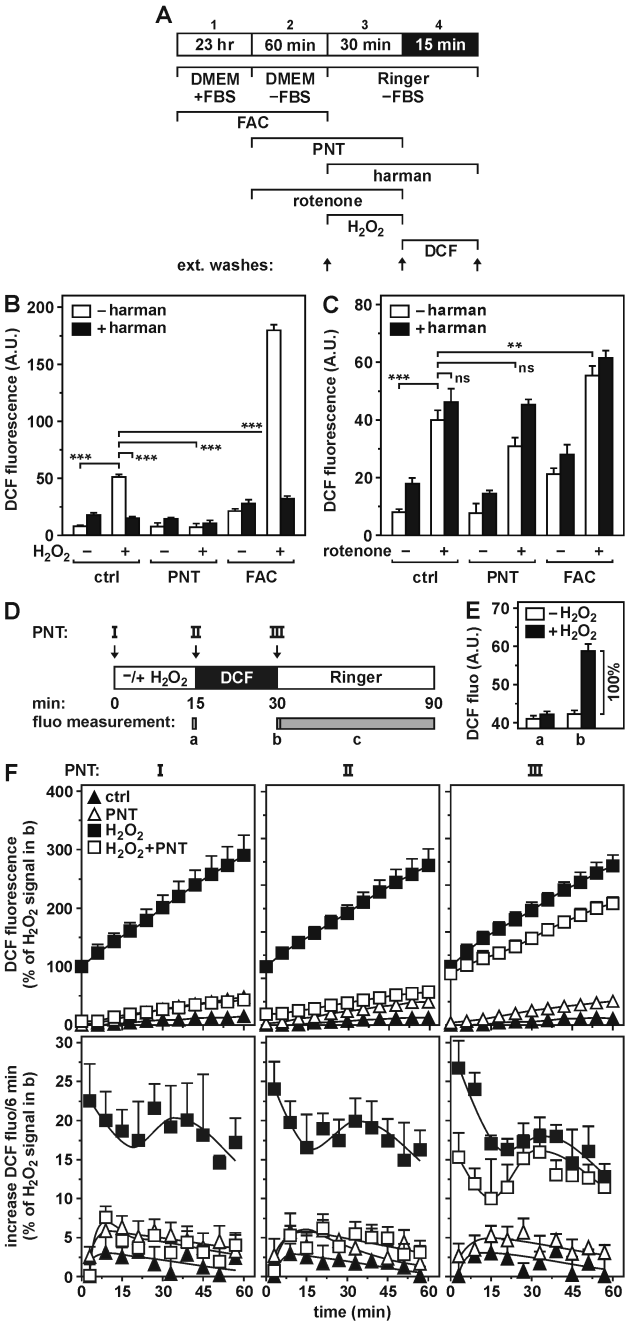
A
1
2
3
4
23 hr
60 min
30 min
15 min
DMEM +FBS
DMEM −FBS
Ringer −FBS
FAC
PNT
harman
rotenone
H2O2
DCF
ext. washes:
B
DCF fluorescence (A.U.)
−harman
+harman
H2O2
ctrl
PNT
FAC
C
DCF fluorescence (A.U.)
−harman
+harman
rotenone
ctrl
PNT
FAC
D
PNT:
I
II
III
−/+ H2O2
DCF
Ringer
min:
0
15
30
90
fluo measurement:
a
b
c
E
DCF fluo (A.U.)
−H2O2
+H2O2
100%
a
b
F
PNT:
I
II
III
ctrl
PNT
H2O2
H2O2+PNT
DCF fluorescence (% of H2O2 signal in b)
increase DCF fluo/6 min (% of H2O2 signal in b)
time (min)

Fig. 7

2',7'-dichlorofluorescin-based analysis of Fenton chemistry reveals auto-amplification of probe fluorescence and albumin as catalyst for the detection of hydrogen peroxide

Teresa Gonzalez, Franck Peiretti, Catherine Defoort, Patrick Borel, and Roland Govers *

Aix Marseille University, INSERM, INRAE, C2VN, 13385 Marseille, France
* Corresponding author; Roland.Govers@univ-amu.fr

SUPPLEMENTARY MATERIAL

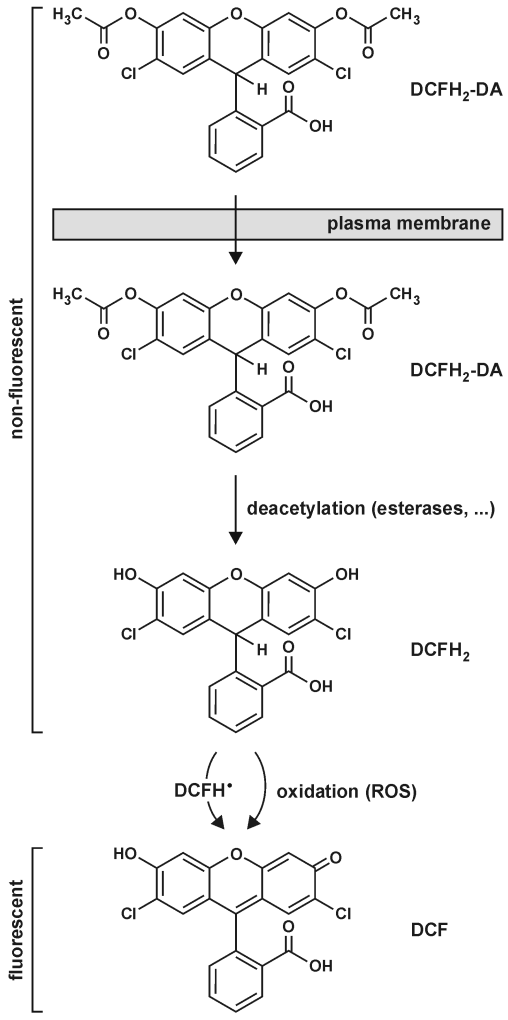

Suppl. Figure S1. Molecular structures of $DCFH_2$-DA, $DCFH_2$, and DCF and their conversion. 2',7'-Dichlorodihydrofluorescein diacetate ($DCFH_2$-DA) penetrates into the cell, where it is converted by cellular esterases into 2',7'-dichlorodihydrofluorescein ($DCFH_2$), which can be oxidized by ROS, leading to the formation of the fluorescent 2',7'-dichlorofluorescein (DCF). The transformation of $DCFH_2$ into DCF involves two subsequent one-electron oxidation reactions, with the DCF radical ($DCFH^{\bullet}$) as intermediate reaction product or a two-electron oxidation reaction. Of note, $DCFH_2$-DA was used throughout the current study in both cell-free experiments as well as in cellular assays but is referred to as 'DCF' throughout the study for the sake of simplicity. $DCFH_2$-DA is deacetylated by esterases and by alcaline hydrolysis, but is also spontaneously deacetylated up to 20% per hour through auto-oxidation [18,38,39], which may possibly be further enhanced under conditions of oxidative stress.

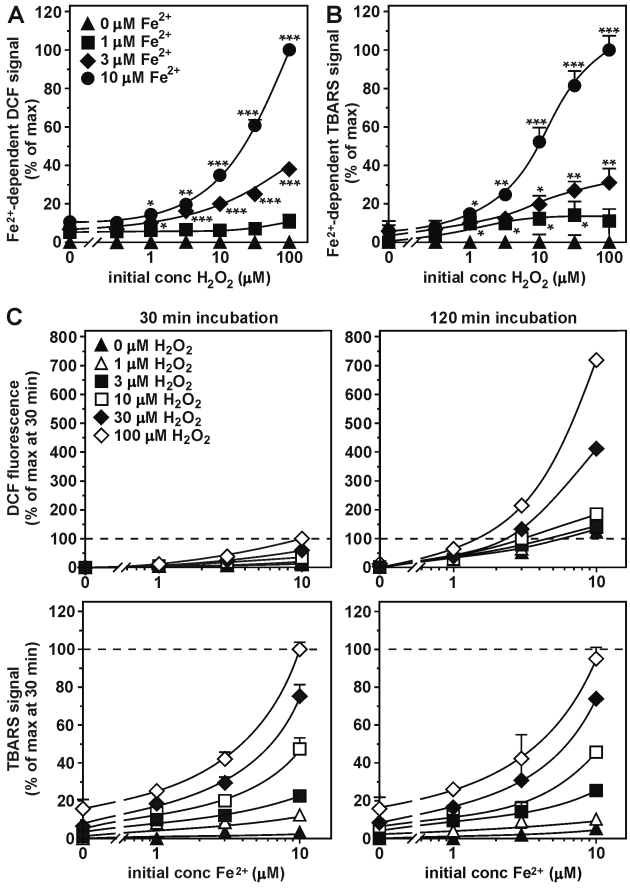

Suppl. Figure S2. Comparison of DCF- and TBARS-mediated measurement of hydroxyl radicals in a protein-free system. (**A,B**) H_2O_2- and Fe^{2+}-dependent oxidative potential was measured by DCF (A) and TBARS (B). The Fe^{2+}-independent signal (i.e. at 0 μM Fe^{2+}) was subtracted for every concentration of H_2O_2 in order to determine Fe^{2+}-dependent signal, representing the net hydroxyl signal. (**C**) DCF (top panels) and TBARS signals (lower panels) were determined after 30 min (left panels) and 120 min at 37°C (right panels) and expressed as percentage of maximum signal at 30 min of incubation (indicated by the dotted lines). Note that DCF but not TBARS signals largely increased between 30 and 120 min. *P<0.05; **P<0.01; ***P<0.001, versus controls at 0 μM H_2O_2.

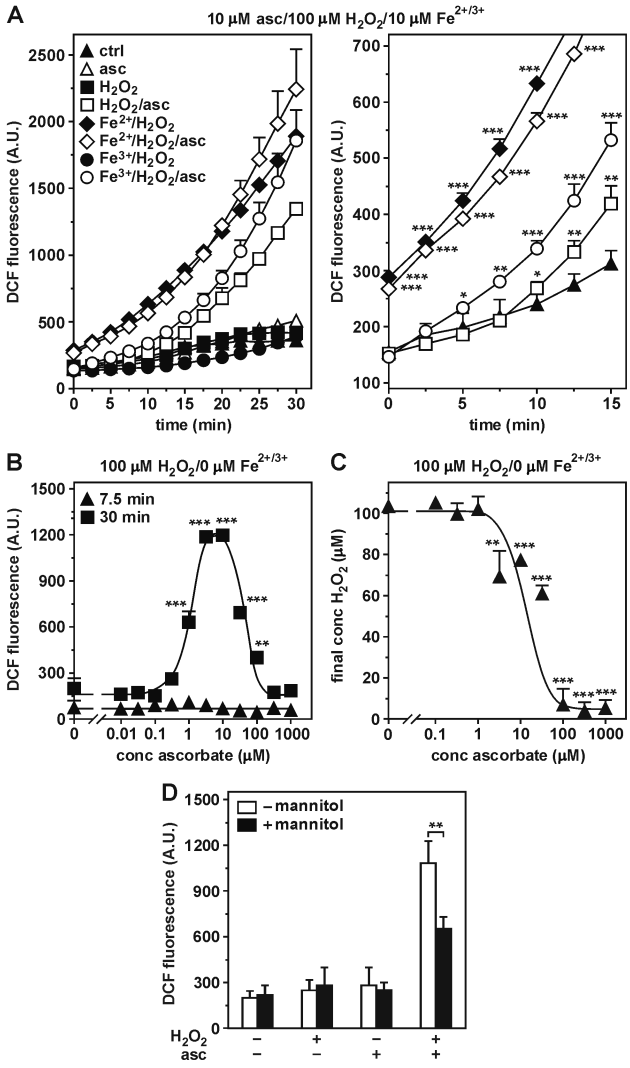

Suppl. Figure S3. Kinetics of iron/H_2O_2- and ascorbate/H_2O_2-induced formation of hydroxyl radicals in a protein-free environment. (A) DCF was incubated for 30 min at 37°C in the absence or presence of 100 µM H_2O_2, 10 µM ascorbate, 10 µM Fe^{2+}, and 10 µM Fe^{3+}. DCF fluorescence was measured every 2.5 min. The right panel displays part of the left panel and demonstrates that while Fe^{2+}/H_2O_2 (filled diamonds) and Fe^{3+}/H_2O_2/ascorbate (open circles) started to generate hydroxyl radicals (i.e. increased DCF fluorescence) within 5 min, the ascorbate/H_2O_2-induced generation of hydroxyl radicals (open squares) was not detectable during the first 7.5 min. **(B)** DCF was incubated for 30 min with 100 µM H_2O_2 and various concentrations of ascorbate in the absence of iron. DCF fluorescence was measured at 7.5 and 30 min. (**C**) After a 30 min incubation of 100 µM H_2O_2 with various concentrations of ascorbate, the remaining concentrations of H_2O_2 were determined. (**D**) DCF was incubated for 30 min in the absence or presence of 100 µM H_2O_2, 10 µM ascorbate, and 100 mM mannitol. DCF fluorescence was measured. *, P<0.05; **, P<0.01; ***, P<0.001, compared with control (A), with incubation without ascorbate (B and C), and with same condition without mannitol (D).

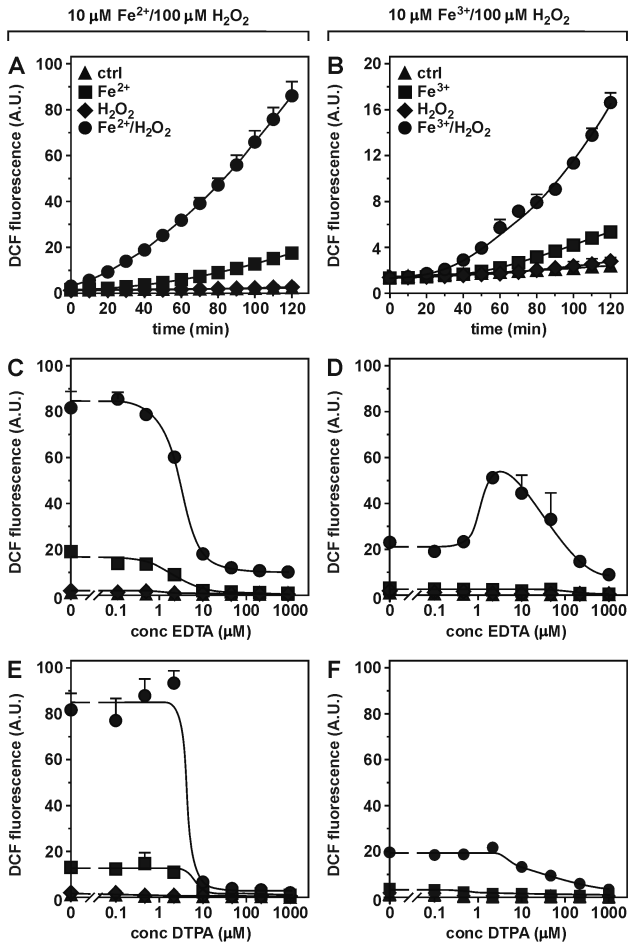

Suppl. Figure S4. Chelator EDTA but not DTPA is capable of enhancing Fe^{3+}/H_2O_2-induced generation of hydroxyl radicals. (**A,B**) DCF was incubated for up to 120 min at 37°C in the absence or presence of 100 μM H_2O_2 and either 10 μM Fe^{2+} (A) or 10 μM Fe^{3+} (B). Fluorescence was measured every 10 min. Of note, while Fe^{2+}/H_2O_2 instantaneously increased DCF fluorescence, Fe^{3+}/H_2O_2 enhanced DCF signal from 40 min onwards. (**C-F**) DCF was incubated for 120 min at 37°C in the absence or presence of 100 μM H_2O_2 and either 10 μM Fe^{2+} (C,E) or 10 μM Fe^{3+} (D,F) with various concentrations of EDTA (C,D) or DTPA (E,F). Increases in DCF fluorescence were measured. Similar fluorescence arbitrary units are depicted for all panels.

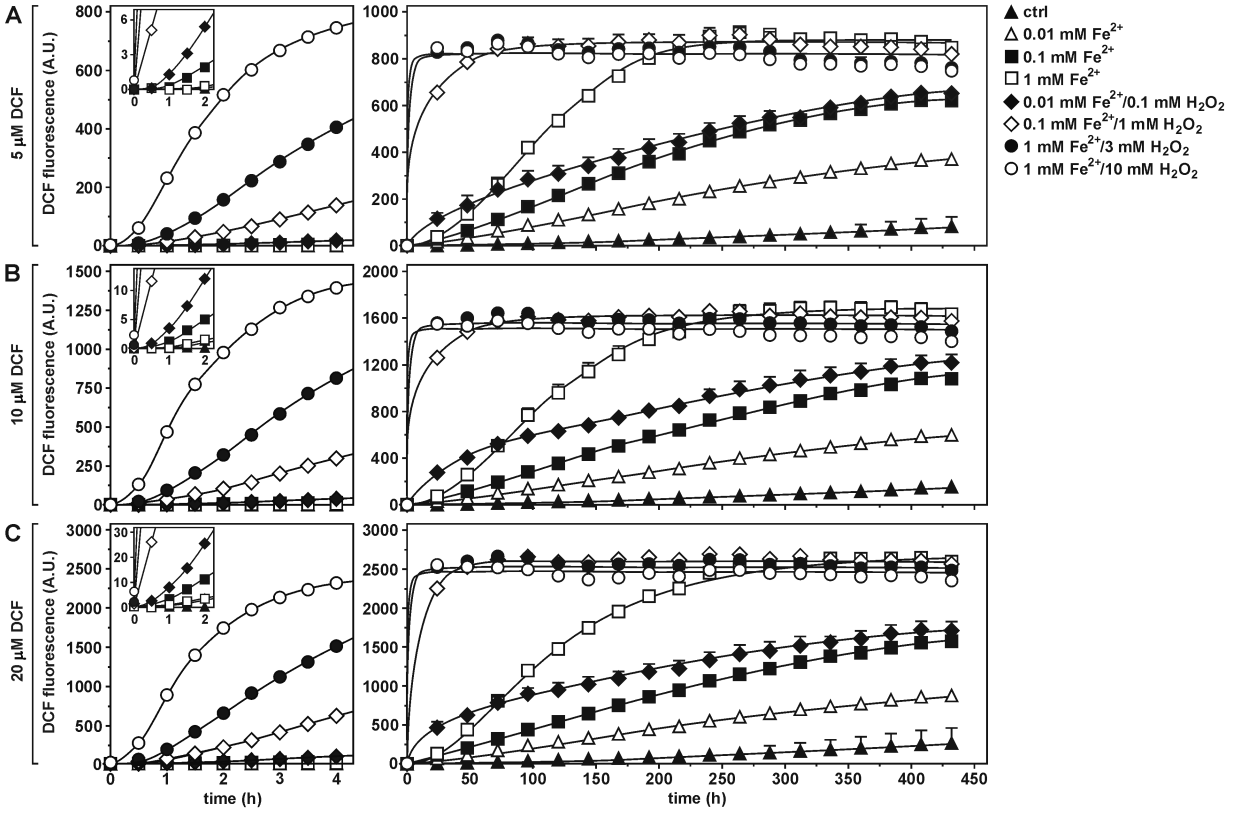

Suppl. Figure S5. Measurement of Fe^{2+}- and Fe^{2+}/H_2O_2-induced DCF fluorescence in the abence of BSA up to plateau levels. DCF, at a concentration of 5 (**A**), 10 (**B**), and 20 µM (**C**), was incubated at 37°C with the indicated concentrations of Fe^{2+} and H_2O_2. Fluorescence was measured every 30 min during the first 4 h (left panels) and every 24 h during 18 days (right panels). Plates were sealed in between daily measurements. The same fluorescence arbitrary units (A.U.) are used for the different panels and also for Suppl. Fig. S6 and S8. Inserts are close-ups of the bottom parts of the panels and show 10 µM Fe^{2+}/100 µM H_2O_2-induced increases in DCF fluorescence (◆). Of note, plateau fluorescence increases with higher concentrations of DCF and plateau fluorescence for all three concentrations of DCF is ~1000 and ~110 times the fluorescence induced by 30 and 120 min of 10 µM Fe^{2+}/100 µM H_2O_2 (◆), respectively (conditions usually used throughout the study).

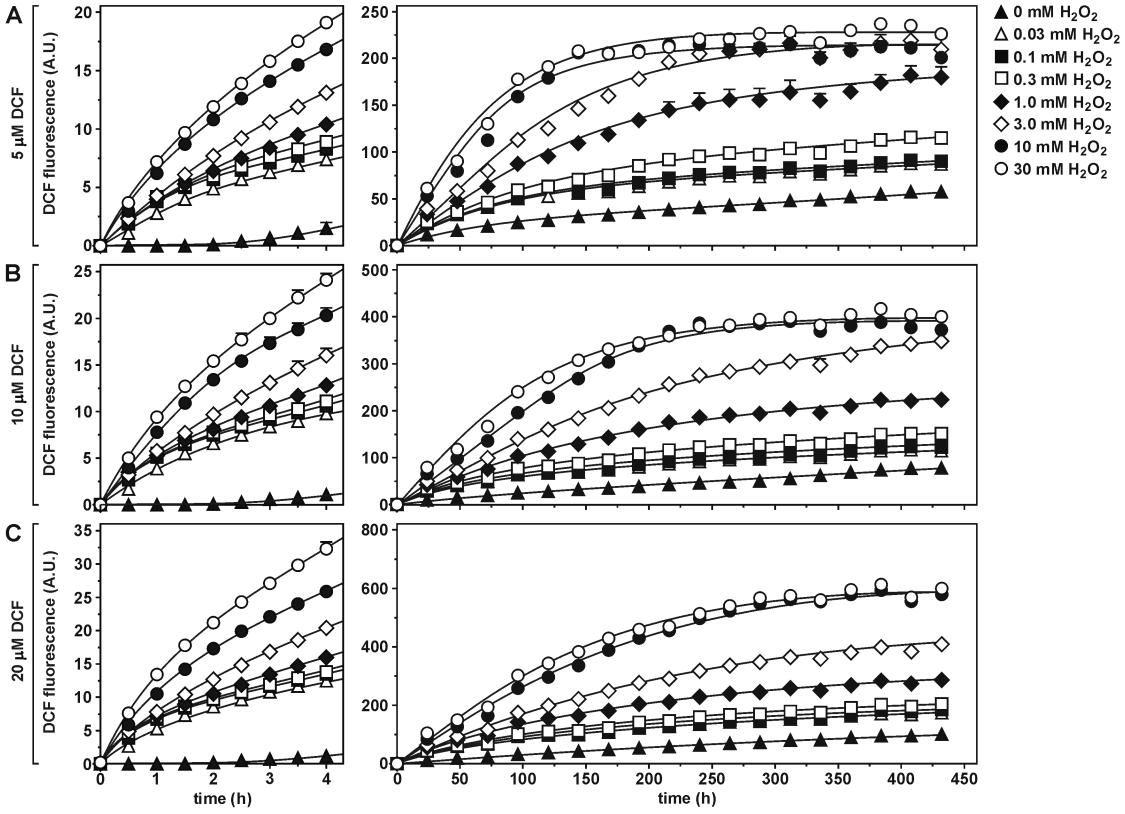

Suppl. Figure S6. Measurement of H_2O_2-induced DCF fluorescence in the presence of 0.2% BSA up to plateau levels. DCF, at a concentration of 5 (**A**), 10 (**B**), and 20 µM (**C**), was incubated at 37°C with the indicated concentrations of H_2O_2. Fluorescence was measured every 30 min during the first 4 h (left panels) and every 24 h during 18 days (right panels). Plates were sealed in between daily measurements. The same fluorescence arbitrary units (A.U.) are used for the different panels and also for Suppl. Fig. S5 and S8. Of note, plateau fluorescence and time required to reach plateau increase with higher concentrations of DCF and plateau fluorescence for all three concentrations of DCF is ~130 times the fluorescence induced by 30 min of 100 µM H_2O_2 (■, conditions usually used throughout the study).

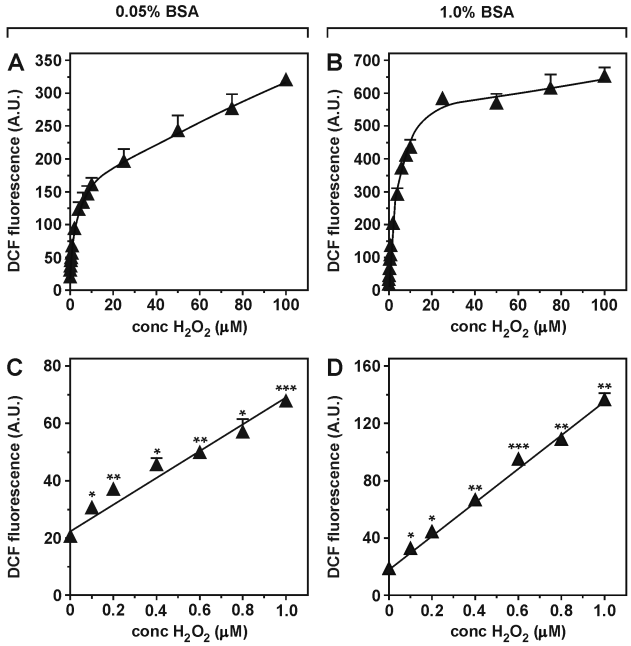

Suppl. Figure S7. H_2O_2 concentration-dependent increases in DCF fluorescence in the presence of BSA. DCF was incubated for 30 min at 37°C with various concentrations of H_2O_2 in the presence of 0.05% (**A,C**) or 1.0% BSA (**B,D**). Of note, while both 0-100 μM H_2O_2 concentration curves are biphasic (A,B), the curves are fully linear up to 1 μM H_2O_2, both in the presence of 0.05% BSA (C, r = 0.984), as well as in the presence of 1% BSA (D, r = 0.998). At both concentrations of BSA, the detection limit for H_2O_2-induced increases in DCF signal was as low as 100 nM. *P<0.05; **P<0.01; ***P<0.001, compared with DCF fluorescence in the absence of H_2O_2.

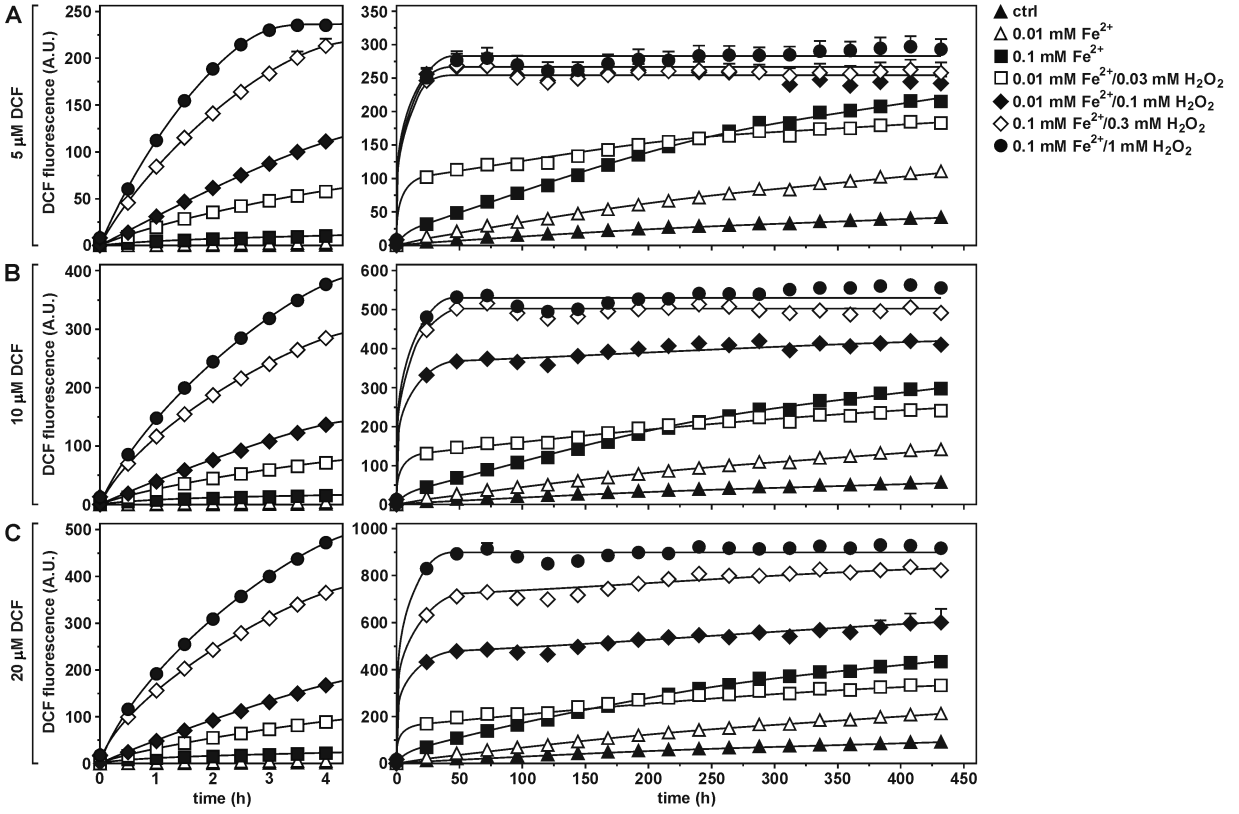

Suppl. Figure S8. Measurement of Fe^{2+}- and Fe^{2+}/H_2O_2-induced DCF fluorescence in the presence of 0.2% BSA up to plateau levels. DCF, at a concentration of 5 (**A**), 10 (**B**), and 20 µM (**C**), was incubated at 37°C with the indicated concentrations of Fe^{2+} and H_2O_2. Fluorescence was measured every 30 min during the first 4 h (left panels) and every 24 h during 18 days (right panels). Plates were sealed in between daily measurements. The same fluorescence arbitrary units (A.U.) are used for the different panels and also for Suppl. Fig. S5 and S6. Of note, plateau fluorescence increases with higher concentrations of DCF and plateau fluorescence is ~20, ~30, and ~40 times the fluorescence induced by a 30 min incubation of 10 µM Fe^{2+}/100 µM H_2O_2 (◆) with 5, 10, and 20 µM DCF, respectively, and ~4, ~7, and ~10 times the fluorescence at 120 min of incubation (conditions usually used throughout the study).

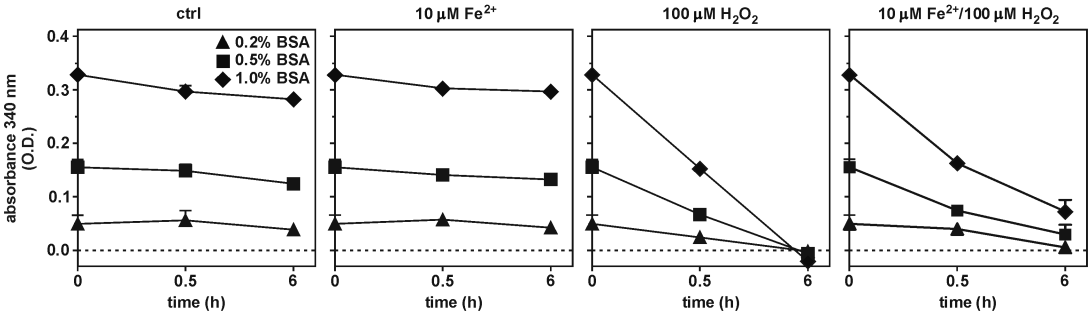

Suppl. Figure S9. Effect of ROS on the free thiol group in BSA. BSA, at a concentration of 0.2, 0.5, and 1.0% (w/v), was incubated for 0.5 or 6 h at 37°C in the absence or presence of 10 µM Fe^{2+} and 100 µM H_2O_2, followed by the addition of DTNB and absorbance measurements to determine the relative amount of remaining free thiol groups. Control BSA samples ('0 h') were not incubated at 37°C nor treated with Fe^{2+} and H_2O_2. Background absorbance was subtracted. Of note, in the presence of H_2O_2 and Fe^{2+}/H_2O_2, the relative amount of free thiol groups in BSA was largely reduced, indicating a chemical reaction of ROS with BSA.

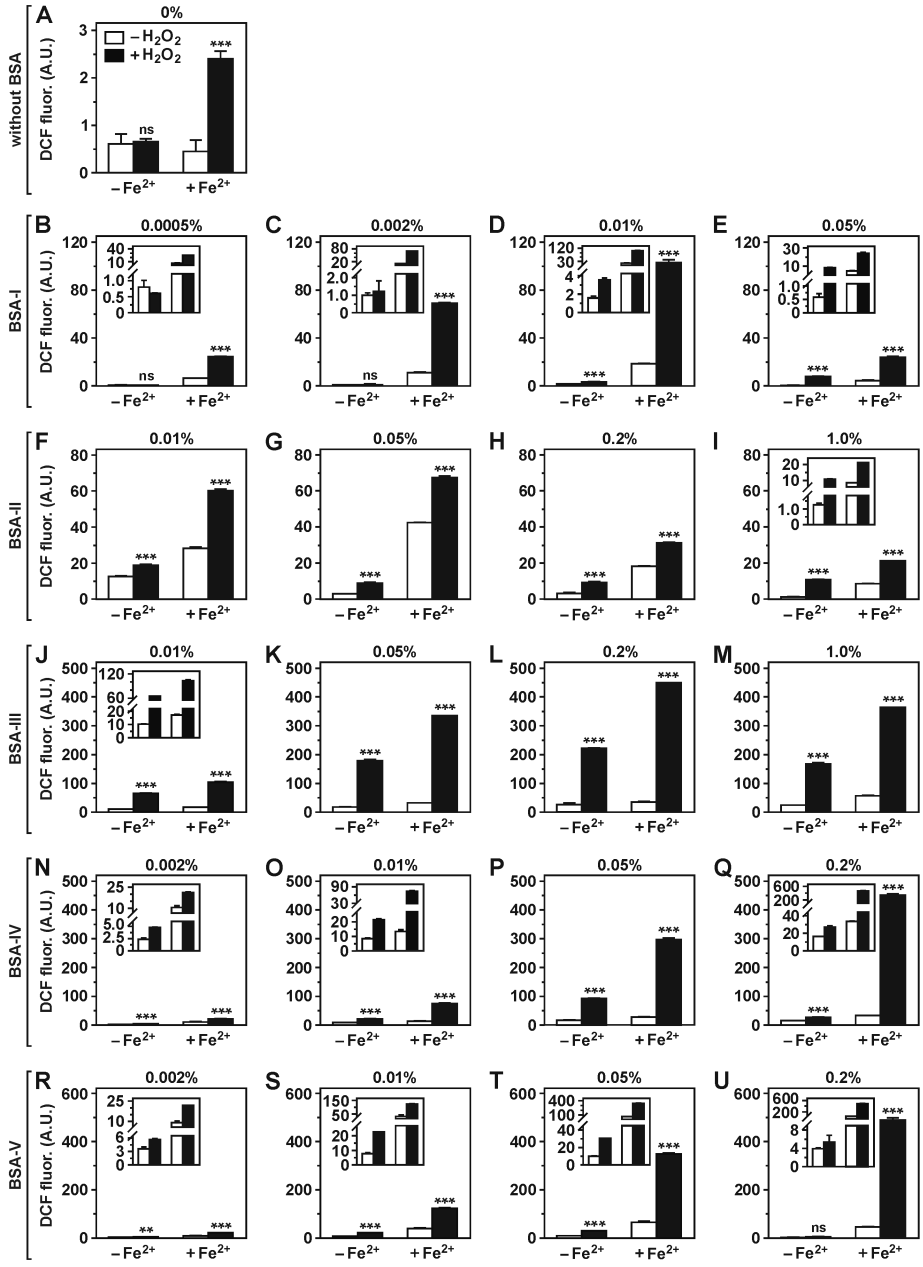

Suppl. Figure S10. Dose-dependent effects of various sources of BSA on DCF fluorescence in the absence or presence of H_2O_2 and Fe^{2+}. DCF was incubated in the absence or presence of 10 μM H_2O_2, 1 μM ferrous iron, and various concentrations of BSA from different sources (see *Materials and Methods*). Increases in DCF fluorescence were measured. The data from this figure were used to calculate the graphs of Fig. 6B. Concentrations of BSA are indicated above the graphs. Similar fluorescence arbitrary units (A.U.) are used for all panels, enabling comparisons between panels. Of note, y-axes are identical for the different concentrations of each BSA, but different between the various BSA batches. For each batch of BSA, the different concentrations were analyzed on the same 96 well plate. *P<0.05; **P<0.01; ***P<0.001, compared with its control without H_2O_2. n.s., non-significant.

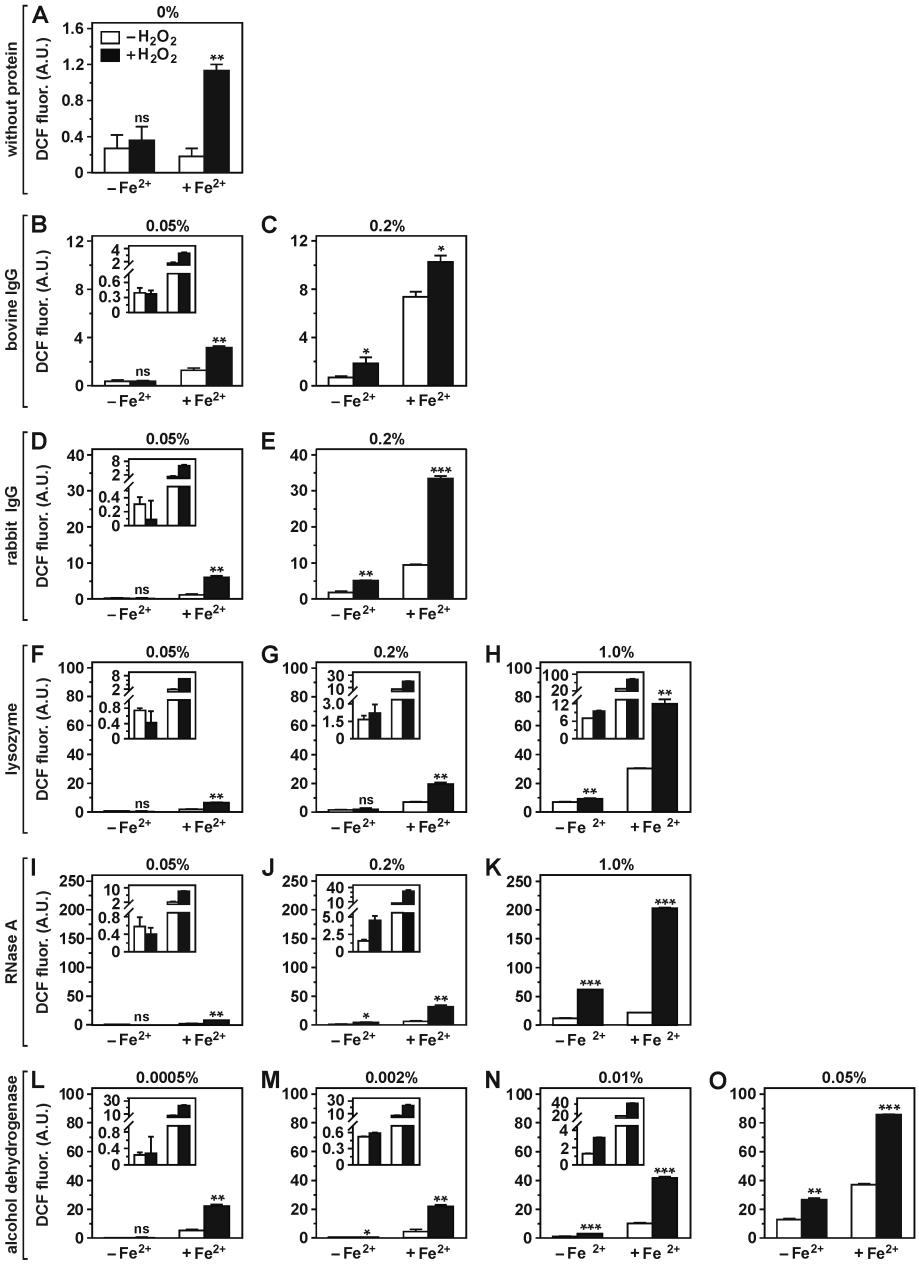

Suppl. Figure S11. Dose-dependent effects of various proteins on DCF fluorescence in the absence or presence of H_2O_2 and Fe^{2+}. DCF was incubated in the absence or presence of 10 μM H_2O_2, 1 μM ferrous iron, and various concentrations of the indicated proteins. Increases in DCF fluorescence were measured. Data from this figure were used to calculate the graphs of Fig. 6C. Protein concentrations are indicated above each graph. Similar fluorescence arbitrary units (A.U.) are used for all data, enabling comparisons between all panels. Y-axes are identical for the different concentrations of each protein, but different between proteins. For each of the proteins tested, the different concentrations where analyzed on the same 96 well plate. *P<0.05; **P<0.01; ***P<0.001, compared with its control without H_2O_2. n.s., non-significant.

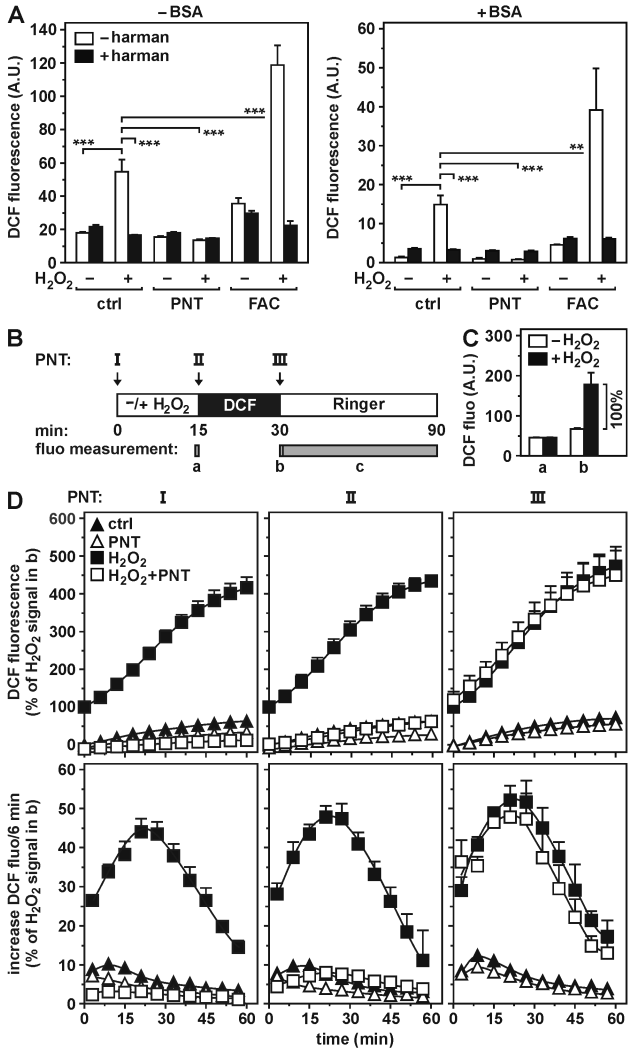

Suppl. Figure S12. DCF fluorescence in H_2O_2-treated cells in the absence of BSA. (A) Adipocytes were incubated with or without 250 µM H_2O_2, 10 µM PNT, 150 µg/ml FAC, and 500 µM harman as indicated (similarly as in Fig. 7A,B), in the absence (left panel) or presence of 0.2% BSA (right panel). Fluorescence was measured before and after DCF incubation (after cell washes) and DCF-specific cellular fluorescence was determined. Similar fluorescence arbitrary units are used for both panels so that fluorescence from both panels can be compared. (**B-D**) Adipocytes were subjected to a similar experiment as in Fig. 7D-F, but in the absence of BSA. After incubating for 1 hour in serum- and BSA-free DMEM, adipocytes were incubated for 90 min in BSA-free Ringer solution that contained 500 µM H_2O_2 during the first 15 min and DCF for the next 15 min. Cells were washed before and after the DCF incubation. PNT (10 µM) or vehicle (DMSO) was included from the beginning of the H_2O_2 incubation ('I'), from the incubation of the cells with DCF ('II') or after the removal of DCF ('III'), as shown in (B). DCF fluorescence of control and H_2O_2-treated cells was measured at points 'a' and 'b' (C). Similar fluorescence arbitrary units are used in C and in Fig 7E, enabling comparison of these graphs. Fluorescence was also measured at 6 min intervals during period 'c', with PNT added at time points I, II, or III, and expressed as percentage of H_2O_2-specific signal in 'b' (D, upper panels). Increases in fluorescence between measurements were calculated and expressed as percentage of H_2O_2-specific signal in 'b' (D, lower panels). *, P<0.05; **, P<0.01; ***, P<0.001.

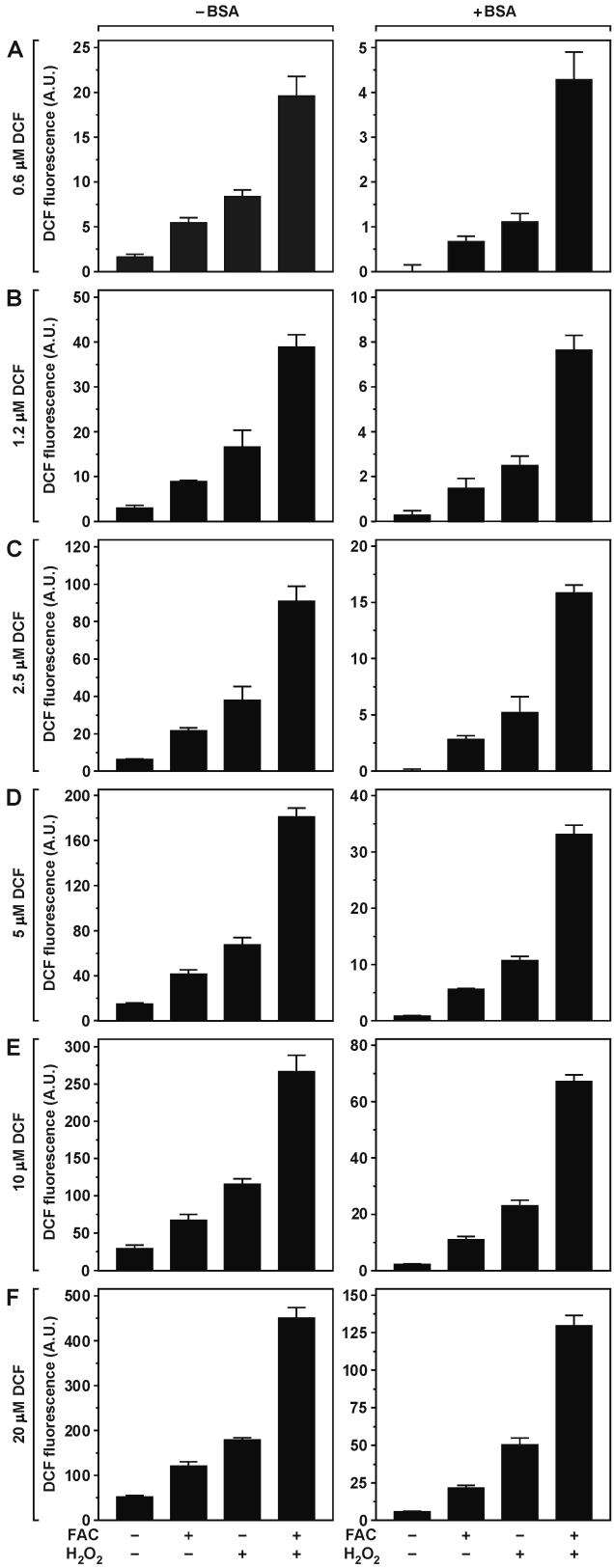

Suppl. Figure S13. Effect of various concentrations of DCF on fluorescence in H_2O_2-treated cells. Adipocytes were incubated for 23 h in DMEM/FBS with or without 150 µg/ml FAC, followed by incubations in Ringer solution in the absence of FBS, without BSA (left panels) or with 0.2% BSA (right panels): for 1 h in the absence or presence of 150 µg/ml FAC, for 30 min in the absence or presence or 250 µM H_2O_2, and for 15 min with 0.6 (A), 1.2 (B), 2.5 (C), 5 (D), 10 (E), or 20 µM DCF. Increases in cellular fluorescence during the final 15 min were measured. Of note, for all panels the relative effects of FAC, H_2O_2, and FAC/H_2O_2 are quite similar. However, compared with incubations without BSA (left panels), incubations with BSA (right panels) show 4 to 6 times less absolute fluorescence and lower relative background fluorescence: background signal in the absence of FAC and H_2O_2 is 0.2-4.3% of FAC/H_2O_2 signal in the presence of BSA and 6.8-11.4% in the absence of BSA. Accordingly, while FAC and H_2O_2 absolute fluorescence signals are highly similar between 0.6 µM DCF in the absence of BSA (A, left panel) and 5 µM DCF in the presence of BSA (D, right panel), absolute background fluorescence is much lower in the presence of BSA.